

N A S A T E C H N I C A L
R E P O R T



NASA TR R-229

C. /

LOAN COPY # 400
AUG 1 1966
KIRTLAND AIR FORCE BASE



PLANE THERMOELASTIC DEFORMATION
OF INTERNALLY HEATED ANNULAR
DISKS OR HOLLOW CYLINDERS

by Franklyn B. Fuller

Ames Research Center
Moffett Field, Calif.

NATIONAL AERONAUTICS AND SPACE ADMINISTRATION • WASHINGTON, D. C.



TECH LIBRARY KAFB, NM



0068509

PLANE THERMOELASTIC DEFORMATION OF INTERNALLY HEATED
ANNULAR DISKS OR HOLLOW CYLINDERS

By Franklyn B. Fuller

Ames Research Center
Moffett Field, Calif.

NATIONAL AERONAUTICS AND SPACE ADMINISTRATION

For sale by the Clearinghouse for Federal Scientific and Technical Information
Springfield, Virginia 22151 - Price \$2.00

PLANE THERMOELASTIC DEFORMATION OF INTERNALLY HEATED
ANNULAR DISKS OR HOLLOW CYLINDERS

By Franklyn B. Fuller
Ames Research Center

SUMMARY

A plane elastic problem of bodies bounded by concentric circles and heated at the inner boundary is solved in the "uncoupled, quasi-static" approximation. The heating takes place by surface heat transfer, with limiting cases corresponding to sudden temperature change and to constant flux of heat. The stress boundary conditions treated are those of constant pressure at the inner wall while the outer wall may be either free or rigidly restrained.

The time-dependent results for stresses, displacement, and temperature are calculated and shown for several cases with varying values for the parameters specifying heat transfer and wall thickness. The effect of varying Poisson's ratio is also examined. Formulas for steady-state distributions of the quantities of interest are also given, as well as some approximate results that can be used for very small times.

INTRODUCTION

There are many engineering uses for cylindrical vessels or annular disks, and some of these involve differential heating of inner and outer cylindrical surfaces with consequent thermal stresses. Some examples are given by Heisler in reference 1. The present work was begun in an effort to calculate the thermoelastic behavior of some disks used in a constricted arc wind tunnel, in which arc-heated gas flows through the central hole of the disks. The formulation of the problem and the subsequent solutions are, however, cast in general terms and the results may be adapted to a variety of specific applications.

The calculation of thermoelastic stresses in circular cylinders has received a good deal of attention in the past, as attested by the contents and/or bibliographies of references 1-8. Most of the earlier work was concerned with the solid cylinder (or disk) and the paper of Jaeger (ref. 9) is a useful collection of numerical and graphical results for that case. Hollow cylinders (or annular disks) have not, however, been so well covered. The early papers of Dahl (ref. 4) and Kent (ref. 7) give analytical results for the present problem, but in reference 4 the numerical results apply to either thin-walled cylinders or to thick-walled ones with special temperature distributions. In reference 7, there are some very brief numerical examples given.

More recently, Trostel (ref. 10) has given a general solution for a hollow circular cylinder of finite length, from which are extracted some results for the infinite-length, or two-dimensional, case. A method for approximate solution of the (two-dimensional) hollow cylinder problem (among others) is set out in reference 11, and the case of a thin-walled cylinder with internal heat generation is treated in reference 12. This list is certainly not exhaustive, but serves to illustrate the fact that there does not seem to be any systematic

presentation of thermoelastic stresses for the two-dimensional body bounded by concentric circles and undergoing various types of heating. This is probably because, as noted in reference 1, there is a new parameter to be considered over those for the solid body, and the resulting analytical expressions are rather formidable unless there is an electronic computer available.

It was therefore considered that an extensive set of calculations of thermal stresses in the two-dimensional elastic case (annular disks or long hollow cylinders) would be useful in several fields of engineering. This is particularly so for the disks with thick walls where approximate results are not so simply derived as for thin walls. The theory to be used in solving this problem is the one aptly called "quasi-static, uncoupled" in reference 2. In this, the dynamic effects of heating, and the effect of volume change on heating, are ignored. As a result of this approximation, the heat-conduction problem can be solved first, and the result used in determining stress. Circumstances under which this decoupling is permissible are discussed in reference 2. There, examples in which more exact solutions are obtainable are analyzed, and some indications as to the size of the error are deduced.

In a rough way, it appears that the quasi-static uncoupled solutions are valid when the product of the combinations

$$\left[3 \frac{E\alpha^2 T_i}{(1-2\nu)\rho c_v} \right] \left(\frac{\dot{e}}{3\alpha T} \right) \ll 1$$

(T_i is the initial, strain-free temperature, ρ the density, c_v the specific heat at constant volume of the material, \dot{e} the rate of volume dilatation, and T the rate of change of temperature. The remaining symbols are defined in the appendix.) The smallness of the second ratio means that pronounced lag between temperature and displacement should not arise, nor should vibrations be induced. (See ref. 2 for a complete discussion.)

The manner of heating the body in question is of some importance. In much of the thermal stress work the initial condition of sudden change of temperature at some surface is taken. The overly conservative design requirements from this condition are pointed out by Nádai (ref. 13, pp. 397-398) and by Heisler (ref. 1). It is more realistic to consider that there is a surface heat-transfer resistance, and to alter the boundary conditions accordingly. This causes some increase in analytic complexity and, as a result, a new parameter appears, namely the Nusselt, or Biot, number which involves the surface heat-transfer coefficient.

Once the transient temperature distribution is known, the stresses may be determined. For the case studied, this amounts to evaluating certain integrals of the temperature distribution (as given, e.g., in ref. 14) together with constants to fit stress boundary conditions. These conditions are here taken to be that there is a fixed pressure acting on the inner surface, while the outer surface may be either free or rigidly restrained. Intermediate cases of elastic restraint can be interpolated between these extremes.

Formulas will be given from which temperature, displacement, and stresses can be calculated for arbitrary position and time. Numerical results which sample the full range of the parameters affecting the character of the solution will be presented and discussed. These should be sufficient for a designer to

obtain estimates for stresses in cases other than those directly shown. Steady-state results are quite simple and are easily calculated for any case of interest.

At the opposite extreme from the steady-state distributions are the initial ones, that is, the temperature and stress distributions which occur shortly after the onset of heating (or cooling). The starting distributions are of considerable interest because the gradients of temperature and hence of stress are most severe then (when there is a surface heat-transfer resistance). They are difficult to calculate by use of the general results, owing to slow convergence of series expansions. However, operational techniques (see Goldstein, ref. 15) lend themselves to approximate calculation of these short-time results, and a number of such formulas are given.

ANALYSIS

As stated in the Introduction, the quasi-static, uncoupled approximation in thermoelasticity will be employed. In this, the temperature distribution is first determined as a solution to the linear heat-conduction equation, and then the temperature function is used to determine displacement and stresses.

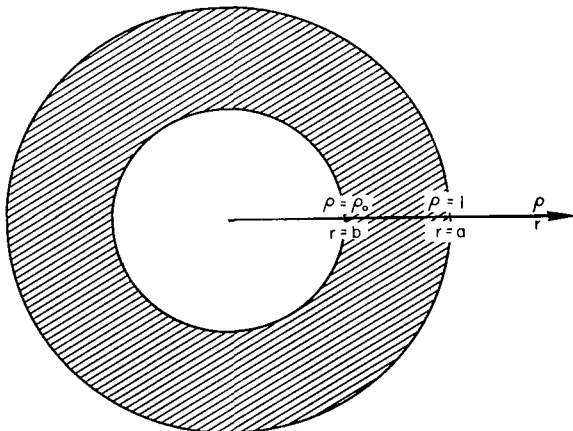
Temperature Distributions

First, the temperature distribution for a region bounded by concentric circular cylindrical surfaces without variation along the axial direction can be written out. The problem is also specialized to allow only radial variation of all quantities. There is to be a choice of three boundary conditions on the temperature or its gradient (flux) at the inner cylindrical surface. The equation of heat conduction is, in the absence of extraneous heat sources,

$$\frac{\partial^2 T}{\partial r^2} + \frac{1}{r} \frac{\partial T}{\partial r} = \frac{1}{\kappa} \frac{\partial T}{\partial t}$$

where the symbols are defined in the appendix. The thermal diffusivity κ is taken to be constant. It will be convenient to introduce the dimensionless variables (see sketch)

$$\rho = a^{-1}r, \quad \rho_0 = a^{-1}b, \quad \tau = \kappa a^{-2}t$$



where a is the outer radius of the disk and b the inner. The equation of conduction becomes

$$\frac{\partial^2 T}{\partial \rho^2} + \frac{1}{\rho} \frac{\partial T}{\partial \rho} = \frac{\partial T}{\partial \tau} \quad (1)$$

As initial condition, always

$$T(\rho, 0) = T_1 \quad (2)$$

where T_1 is a temperature at which the material is strain free. A boundary condition at the outer surface $r = a$, hence at $\rho = 1$, is always to be

$$T(1, \tau) = T_1 \quad (3)$$

The boundary condition at the inner surface, $r = b$, or $\rho = \rho_0$, will be one of three:

Case A $T(\rho_0, \tau) = T_0 \quad (4a)$

Case B $-k \frac{\partial T}{\partial \rho} \Big|_{\rho=\rho_0} = aF_0 \quad (4b)$

where F_0 is the heat flux,

Case C
$$\left. -k \frac{\partial T}{\partial \rho} \right|_{\rho=\rho_0} = ha \left[T_0 - T(\rho_0, \tau) \right] \quad \right\} \quad (4c)$$

or
$$\left. \frac{\partial T}{\partial \rho} \right|_{\rho=\rho_0} = - \frac{m}{\rho_0} \left[T_0 - T(\rho_0, \tau) \right]$$

where h is the surface heat-transfer coefficient and $m (= hb/k)$ is the Biot number. The boundary conditions are here taken to be independent of time, for $t > 0$. More complicated time variations can be treated by use of Duhamel's theorem (ref. 16) or by direct use of the convolution process for Laplace transforms. In the last boundary condition, C, let $m \rightarrow \infty$. Then the flux may be loosely considered as becoming infinite such that the temperature at $\rho = \rho_0$ jumps suddenly to T_0 at $t = 0$, and thereafter remains at T_0 . Thus, this limit corresponds to case A. On the other hand, if the boundary conductance $h \rightarrow 0$ while the reservoir temperature T_0 becomes very large, it can be thought, again rather loosely, that this corresponds to case B, with constant flux. Thus, when a solution for case C has been obtained, the two limiting cases $m = \infty, 0$ should lead to solutions for cases A and B, respectively. This can, of course, be checked by actual calculation.

The problem posed in equations (1) to (4) can be solved by standard techniques; in fact, a solution for a more general problem, from which the present one can be derived, is given in reference 16. However, in view of the need which will arise later for the Laplace transform of the solution, it is convenient to go very briefly through the process. The Laplace transform of a function is here denoted by a bar, thus

$$\bar{f}(p) = \int_0^\infty e^{-p\tau} f(\tau) d\tau$$

In terms of these new variables \bar{T} and p , it is now necessary to solve the differential equation

$$\frac{d^2\bar{T}}{dp^2} + \frac{1}{p} \frac{d\bar{T}}{dp} - q^2\bar{T} = -T_1 \quad (1a)$$

where

$$q^2 = p$$

and to make the solution conform to the appropriate boundary conditions at $p = \rho_0, 1$. The last equation is recognized as Bessel's for modified functions of order zero. The complete solution is then

$$\bar{T} = A I_0(q\rho) + B K_0(q\rho) + p^{-1} T_1$$

where I_0, K_0 denote the modified Bessel functions of first and second kind as defined by Watson (ref. 17). The determination of the constants A, B is made by means of boundary conditions; only condition C (eq. (4c)) will be considered for this purpose. The result is the transform

$$\frac{\frac{T_C - T_1}{T_0 - T_1}}{m} = -\frac{m}{p} \cdot \frac{I_0(q\rho)K_0(q) - K_0(q\rho)I_0(q)}{I_0(q)\left[\rho_0 q K_0'(q\rho_0) - m K_0(q\rho_0)\right] - K_0(q)\left[\rho_0 q I_0'(q\rho_0) - m I_0(q\rho_0)\right]} \quad (5)$$

Inversion of this transform requires knowledge of the zeros of the denominator in the complex p plane. The pole at $p = 0$ will contribute the steady-state result for the present problem, which is seen to be nonzero by physical reasoning. It is

$$\begin{aligned} \frac{T_C(\rho, \infty) - T_1}{T_0 - T_1} &= \lim_{p \rightarrow 0} m \frac{I_0(q\rho)K_0(q) - K_0(q\rho)I_0(q)}{I_0(q)\left[\rho_0 q K_0'(q\rho_0) - m K_0(q\rho_0)\right] - K_0(q)\left[\rho_0 q I_0'(q\rho_0) - m I_0(q\rho_0)\right]} \\ &= \frac{m \log(1/\rho)}{1 + m \log(1/\rho_0)} \end{aligned} \quad (5a)$$

The remaining zeros of the denominator in equation (5) are real and simple. If they are denoted

$$q = e^{\pm i \frac{\pi}{2} \mu_n}; \quad p = -\mu_n^2$$

and the complex inversion formula

$$\frac{T_C - T_1}{T_O - T_1} = \frac{1}{2\pi i} \int_{\gamma-i\infty}^{\gamma+i\infty} e^{pt} \left(\frac{T_C - T_1}{T_O - T_1} \right) dp , \quad \gamma > 0$$

is used, then after some algebra, and use of relations for the Bessel functions from reference 17, it is found that

$$\begin{aligned} \frac{T_C - T_1}{T_O - T_1} &= \frac{m \log(1/\rho)}{1 + m \log(1/\rho_O)} \\ &+ m\pi \sum_{n=1}^{\infty} e^{-\mu_n^2 \tau} \frac{J_0(\mu_n) \left[\rho_O \mu_n J_1(\rho_O \mu_n) + m J_0(\rho_O \mu_n) \right] \left[J_0(\rho \mu_n) Y_O(\mu_n) - Y_O(\rho \mu_n) J_0(\mu_n) \right]}{\left[\rho_O \mu_n J_1(\rho_O \mu_n) + m J_0(\rho_O \mu_n) \right]^2 - (m^2 + \rho_O^2 \mu_n^2) J_0^2(\mu_n)} \end{aligned} \quad (6)$$

The eigenvalues μ_n are determined from the equation

$$\frac{J_0(\mu_n)}{Y_O(\mu_n)} = \frac{m J_0(\rho_O \mu_n) + \rho_O \mu_n J_1(\rho_O \mu_n)}{m Y_O(\rho_O \mu_n) + \rho_O \mu_n Y_1(\rho_O \mu_n)} \quad (6a)$$

From the result for the mixed boundary conditions, case C, given in equation (6), the results for cases A and B (see eqs. (4a) and (4b)) can now be obtained. First, to obtain case A, m is allowed to become very large, giving, in the limit

$$\frac{T_A - T_1}{T_O - T_1} = \frac{\log\left(\frac{1}{\rho}\right)}{\log\left(\frac{1}{\rho_O}\right)} + \pi \sum_{n=1}^{\infty} e^{-\alpha_n^2 \tau} \frac{J_0(\alpha_n) J_0(\rho_O \alpha_n) [J_0(\rho \alpha_n) Y_O(\alpha_n) - Y_O(\rho \alpha_n) J_0(\alpha_n)]}{J_0^2(\rho_O \alpha_n) - J_0^2(\alpha_n)} \quad (7)$$

where

$$\frac{J_0(\alpha_n)}{Y_O(\alpha_n)} = \frac{J_0(\rho_O \alpha_n)}{Y_O(\rho_O \alpha_n)} \quad (7a)$$

and α_n is written for the typical eigenvalue in this case to distinguish it from that for case C.

To determine the solution for case B, write $m = h(b/k)$ and allow the product $h(T_O - T_1) = m(T_O - T_1)/(b/k)$ to approach unity (corresponding to $(aF_O) = 1$ in eq. (4b)) while $h \rightarrow 0$. Then,

$$\frac{T_B - T_1}{b/k} = \log \frac{1}{\rho} + \pi \sum_{n=1}^{\infty} e^{-\beta n^2 \tau} \frac{J_0(\beta_n) J_1(\rho \beta_n) [J_0(\rho \beta_n) Y_0(\beta_n) - Y_0(\rho \beta_n) J_0(\beta_n)]}{\rho \beta_n [J_1^2(\rho \beta_n) - J_0^2(\beta_n)]} \quad (8)$$

where

$$\frac{J_0(\beta_n)}{Y_0(\beta_n)} = \frac{J_1(\rho \beta_n)}{Y_1(\rho \beta_n)} \quad (8a)$$

Determination of Displacement and Stresses

When the temperature distribution in the material is known, it is possible to calculate the displacement u and the stresses σ_r , σ_θ . Because of the radial symmetry, the shearing stress $\tau_{r\theta}$ vanishes everywhere. On this account, the maximum shear stress at any point is simply $(1/2)|\sigma_r - \sigma_\theta|$.

Plane stress.- If a body is thin, as a plate, in one dimension (say z), and all the forces and stresses lie in the plane of the body, a two-dimensional problem results, in that all stresses σ_z , σ_{yz} , σ_{xz} vanish and the remainder are free of z : (See ref. 1-.) The formulas for displacement and stresses are then (ref. 14)

$$u = \frac{1+\nu}{r} \int_b^r \alpha(T - T_1)x \, dx + C_1 r + C_2 r^{-1} \quad (9a)$$

$$\sigma_r = -\frac{E}{r^2} \int_b^r \alpha(T - T_1)x \, dx + \frac{E}{1-\nu^2} \left[C_1(1+\nu) - C_2 \frac{1-\nu}{r^2} \right] \quad (9b)$$

$$\sigma_\theta = \frac{E}{r^2} \int_b^r \alpha(T - T_1)x \, dx - E\alpha(T - T_1) + \frac{E}{1-\nu^2} \left[C_1(1+\nu) + C_2 \frac{1-\nu}{r^2} \right] \quad (9c)$$

The constants C_1 and C_2 in equations (9) are to be determined by means of stress boundary conditions. As mentioned above, these will be such that there is a pressure p_o acting at the inner surface $r = b$, while the outer surface, $r = a$, is to be either stress free or rigidly restrained. For the first case, that of free outer surface, the constants are to be determined by means of

$$\begin{aligned} \sigma_r &= -p_o & \text{at } r = b \\ \sigma_r &= 0 & \text{at } r = a \end{aligned}$$

Now write

$$\frac{u}{\alpha(T_O - T_1)a} = \frac{1 + \nu}{\rho} I(\rho, \rho_O; \tau) + D_1 \rho + \frac{D_2}{\rho} \quad (10a)$$

$$\frac{\sigma_r}{\alpha(T_O - T_1)E} = - \frac{1}{\rho^2} I(\rho, \rho_O; \tau) + \frac{1}{1 - \nu^2} \left[(1 + \nu) D_1 - (1 - \nu) \frac{D_2}{\rho^2} \right] \quad (10b)$$

$$\frac{\sigma_\theta}{\alpha(T_O - T_1)E} = \frac{1}{\rho^2} I(\rho, \rho_O; \tau) - \frac{T - T_1}{T_O - T_1} + \frac{1}{1 - \nu^2} \left[(1 + \nu) D_1 + (1 - \nu) \frac{D_2}{\rho^2} \right] \quad (10c)$$

where

$$I(\rho, \rho_O; \tau) = \int_{\rho_O}^{\rho} \frac{T(\rho_1, \tau) - T_1}{T_O - T_1} \rho_1 d\rho_1 \quad (10d)$$

The above boundary conditions give

$$D_1 = (1 - \nu) \frac{\rho_O^2 p_O^* + I(1, \rho_O; \tau)}{1 - \rho_O^2}$$

$$D_2 = (1 + \nu) \rho_O^2 \frac{p_O^* + I(1, \rho_O; \tau)}{1 - \rho_O^2}$$

where

$$p_O^* = \frac{p_O}{\alpha(T_O - T_1)E}$$

If the quantities on the left in equations (10a) through (10c) are denoted by u^* , σ_r^* , σ_θ^* for the present case of stress-free outer boundary, there results

$$\begin{aligned} u^* &= \frac{1 + \nu}{\rho} I(\rho, \rho_O; \tau) + \frac{I(1, \rho_O; \tau)}{1 - \rho_O^2} \left[(1 - \nu)\rho + (1 + \nu) \frac{\rho_O^2}{\rho} \right] \\ &\quad + \frac{\rho_O^2 p_O^*}{1 - \rho_O^2} \left[(1 - \nu)\rho + \frac{1 + \nu}{\rho} \right] \end{aligned} \quad (11a)$$

$$\sigma_r^* = -\frac{1}{\rho^2} I(\rho, \rho_o; \tau) + \frac{I(1, \rho_o; \tau)}{1 - \rho_o^2} \left(1 - \frac{\rho_o^2}{\rho^2}\right) + \frac{\rho_o^2 p_o^*}{1 - \rho_o^2} \left(1 - \frac{1}{\rho^2}\right) \quad (11b)$$

$$\sigma_\theta^* = -\sigma_r^* - \frac{T - T_1}{T_o - T_1} + 2 \frac{I(1, \rho_o; \tau)}{1 - \rho_o^2} + 2 \frac{\rho_o^2 p_o^*}{1 - \rho_o^2} \quad (11c)$$

Next, the boundary conditions of rigid restraint of the outer surface and pressure p_o on the inner surface give

$$D_1 = -(1 - \nu^2) \rho_o^2 \frac{p_o^* + I(1, \rho_o; \tau)}{(1 - \nu) + (1 + \nu) \rho_o^2}$$

$$D_2 = (1 + \nu) \rho_o^2 \frac{(1 - \nu) p_o^* - (1 + \nu) I(1, \rho_o; \tau)}{(1 - \nu) + (1 + \nu) \rho_o^2}$$

Denote now the quantities on the left in equations (10) by u' , σ_r' , σ_θ' . Then

$$u' = \frac{1 + \nu}{\rho} I(\rho, \rho_o; \tau) - (1 + \nu) \frac{I(1, \rho_o; \tau)}{(1 - \nu) + (1 + \nu) \rho_o^2} \left[(1 - \nu) \rho + (1 + \nu) \frac{\rho_o^2}{\rho} \right] \\ + \frac{\rho_o^2 (1 - \nu^2) p_o^*}{(1 - \nu) + (1 + \nu) \rho_o^2} \left(\frac{1}{\rho} - \frac{1}{\rho_o} \right) \quad (12a)$$

$$\sigma_r' = -\frac{1}{\rho^2} I(\rho, \rho_o; \tau) + \frac{(1 + \nu) I(1, \rho_o; \tau)}{(1 - \nu) + (1 + \nu) \rho_o^2} \left(\frac{\rho_o^2}{\rho^2} - 1 \right) \\ - \frac{\rho_o^2 p_o^*}{(1 - \nu) + (1 + \nu) \rho_o^2} \left[(1 + \nu) + \frac{1 - \nu}{\rho^2} \right] \quad (12b)$$

$$\begin{aligned}\sigma_{\theta}' &= -\sigma_r' - \frac{T - T_1}{T_o - T_1} - 2(1 + \nu) \frac{\rho_o^2 I(l, \rho_o; \tau)}{(1 - \nu) + (1 + \nu)\rho_o^2} \\ &\quad - 2(1 + \nu) \frac{\rho_o^2 p_o^*}{(1 - \nu) + (1 + \nu)\rho_o^2} \quad (12c)\end{aligned}$$

It is interesting to note that when the outer boundary is free, the stresses σ_r^* , σ_θ^* do not depend upon the Poisson's ratio ν . This is not true for σ_r' and σ_θ' , that is, when the outer boundary is rigidly restrained. In either case, however, the radial displacement does depend upon the Poisson's ratio.

Plane strain. - Here the idealization is that of a long body in which all quantities are independent of axial distance. In this situation, there are axial stresses σ_z acting at the ends of the cylinder of magnitude

$$\sigma_z = \sigma_r + \sigma_\theta$$

These can be removed by a uniform axial stress applied so that the resultant force on the ends is zero. By Saint Venant's principle, this self-equilibrating system acting on the ends will affect only locally the stresses in the cylinder (see ref. 14).

In order to obtain formulas for plane strain problems from the above results for plane stress, it is only necessary to substitute $E/(1 - \nu^2)$, $\nu/(1 - \nu)$, $(1 + \nu)\alpha$ for E , ν , α , respectively. Thus, for example, equation (11b) becomes, for plane strain,

$$\begin{aligned}\sigma_r^* &= \frac{1}{(1 - \nu)} \left[-\frac{1}{\rho^2} I(\rho, \rho_o; \tau) + \frac{I(l, \rho_o; \tau)}{1 - \rho_o^2} \left(1 - \frac{\rho_o^2}{\rho^2} \right) + \frac{\rho_o^2 p_o^*}{1 - \rho_o^2} \left(1 - \frac{1}{\rho^2} \right) \right] \\ &= \frac{\sigma_r}{\alpha(T_o - T_1)E}\end{aligned}$$

The Steady-State Distributions

In all cases, the steady-state temperature distributions are represented by the formula

$$\frac{T(\rho, \infty) - T_1}{T_{ref}} = N \log \frac{1}{\rho} \quad (13)$$

For the three heating modes the constants take the following values:

$$\text{Case A} \quad T_{\text{ref}} = T_0 - T_1; \quad N = \left(\log \frac{1}{\rho_0} \right)^{-1}$$

$$\text{Case B} \quad T_{\text{ref}} = b/k; \quad N = 1$$

$$\text{Case C} \quad T_{\text{ref}} = T_0 - T_1; \quad N = m \left[1 + m \log \left(\frac{1}{\rho_0} \right) \right]^{-1}$$

These temperatures therefore decrease monotonically between $\rho = \rho_0$ and $\rho = 1$. The stresses, as given in equations (10), depend upon the integral

$$I(\rho, \rho_0; \infty) = \int_{\rho_0}^{\rho} \frac{T(\rho_1, \infty) - T_1}{T_{\text{ref}}} \rho_1 d\rho_1 = \frac{N}{2} \left[\rho^2 \log \rho - \rho_0^2 \log \rho_0 - \frac{1}{2} (\rho^2 - \rho_0^2) \right] \quad (14)$$

It is interesting to determine whether the steady-state stresses have an extremum in the interval $\rho_0 < \rho < 1$.

Consider first the stresses as given in equations (10) before any stress boundary conditions are imposed. Then,

$$\frac{1}{\alpha T_{\text{ref}} E} \frac{d\sigma_r}{d\rho} = \frac{2}{\rho^3} I(\rho, \rho_0; \infty) - \frac{N}{\rho} \log \rho + \frac{2}{\rho^3} \frac{D_2}{1 + \nu}$$

$$\frac{1}{\alpha T_{\text{ref}} E} \frac{d\sigma_\theta}{d\rho} = - \frac{2}{\rho^3} I(\rho, \rho_0; \infty) + \frac{N}{\rho} \log \rho + \frac{N}{\rho} - \frac{2}{\rho^3} \frac{D_2}{1 + \nu}$$

An extremum of σ_r occurs at $\rho = \rho_{\text{cr}}$ where

$$\rho_{\text{cr}}^2 = \rho_0^2 \left(1 + \log \frac{1}{\rho_0^2} \right) + \frac{4}{N} \frac{D_2}{1 + \nu} \quad (15)$$

When the value of D_2 found above for a stress-free boundary is used,

$$\rho_{\text{cr}}^{*2} = \frac{\rho_0^2}{1 - \rho_0^2} \left(\log \frac{1}{\rho_0^2} + 4 \frac{\rho_0^*}{N} \right) \quad (15a)$$

It is interesting to note that when the internal pressure is neglected, the critical point for σ_r in the free outer boundary problem is completely independent of all elastic and thermal parameters, depending only on the geometrical quantity ρ_o , the ratio of inner to outer radii of the body. Also, since both p_o^* and N are positive quantities (when $T_{ref} > 0$), it is seen from equation (15a) that a sufficiently high internal pressure p_o can cause the position of the extremum, $\rho = \rho_{cr}$, to move beyond $\rho = 1$.

Examination of the derivative of circumferential stress indicates that no ρ in $\rho_o < \rho < 1$ gives an extremum. Hence, the (algebraically) largest and smallest values of circumferential stress must occur at the boundaries, at least in the steady state.

In the event that the outer boundary is rigidly restrained, equation (15) gives for the critical radius

$$\rho_{cr}^2 = 2\rho_o^2 \frac{1 + (1 - \nu) \log\left(\frac{1}{\rho_o}\right) + \frac{2(1 - \nu)p_o^*}{N}}{(1 - \nu) + (1 + \nu)\rho_o^2} \quad (16)$$

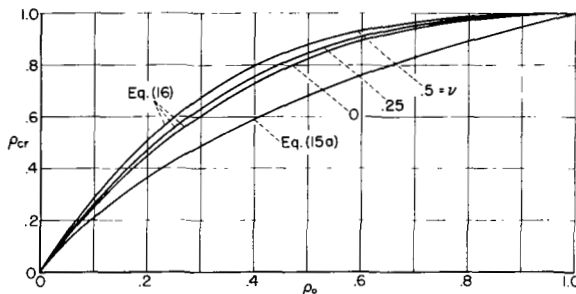


Figure 1.- Locations of extreme values of radial stress in the steady state (eqs. (15) and (16)).

Again the circumferential steady-state stress is monotonic in $\rho_o < \rho < 1$. With the rigidity condition, the value of ρ_{cr} , the position of an interior extremum of radial stress, does depend upon Poisson's ratio ν , even when the internal pressure p_o is ignored.

In figure 1 ρ_{cr} is plotted for free and for rigid outer boundaries. The latter are drawn for three values of the Poisson ratio ν , and p_o is always taken to be zero. It is seen that the effect of change of Poisson ratio is not great, even over the extreme range $0 < \nu < 0.5$.

Initial Behavior of Solutions

The series derived above as solutions for the temperatures and their integrals which are used to determine stresses are not well adapted for use with small values of the "time" τ , say for $\tau < 10^{-2}$. The damping effect of the exponential terms is then delayed, and many terms of the series must be evaluated. Although this is not a serious disadvantage when the summations are calculated by an electronic computer, it is often useful to have a simple expression for the initial behavior of a solution. The applicability of the present results is thereby enhanced since cases not covered by the specific calculations given later may be treated. The eventual distributions in the steady state are known from the previous section.

A particularly advantageous way of obtaining the small τ results was popularized by Goldstein (ref. 15). This involves the use of asymptotic expansions of the Laplace transforms (Goldstein used operational concepts) of the various functions of interest, followed by term-by-term inversion of the results. A discussion of the process, with justification, can be found in reference 18.

Approximations for the temperature.- To start, consider the result given in equation (5) for the Laplace transform of temperature:

$$\frac{T_C - T_1}{T_O - T_1} = \frac{m}{P} \frac{B_O(q\rho)}{mB_O(q\rho_O) - q\rho_O B_1(q\rho_O)} \quad (17)$$

where

$$\left. \begin{aligned} B_O(z) &= I_O(z)K_O(q) - K_O(z)I_O(q) \\ B_1(z) &= I_1(z)K_O(q) + K_1(z)I_O(q) \\ &= B_O'(z) \end{aligned} \right\} \quad (17a)$$

The asymptotic formulae for the modified Bessel functions will be needed; from reference 17,

$$\left. \begin{aligned} I_O(\omega) &\sim \frac{e^\omega}{\sqrt{2\pi\omega}} \left(1 + \frac{1}{8\omega} \right) \\ I_1(\omega) &\sim \frac{e^\omega}{\sqrt{2\pi\omega}} \left(1 - \frac{3}{8\omega} \right) \\ K_O(\omega) &\sim \pi \frac{e^{-\omega}}{\sqrt{2\pi\omega}} \left(1 - \frac{1}{8\omega} \right) \\ K_1(\omega) &\sim \pi \frac{e^{-\omega}}{\sqrt{2\pi\omega}} \left(1 + \frac{3}{8\omega} \right) \end{aligned} \right\} \quad (18)$$

where terms $O(1/\omega^2)$ in the parentheses have been dropped. From these results, the quantities B_O, B_1 can be found:

$$\left. \begin{aligned} B_0(\omega) &\sim -\frac{1}{2\sqrt{q\omega}} \left\{ e^{(q-\omega)} \left[1 - \frac{1}{8} \left(\frac{1}{\omega} - \frac{1}{q} \right) \right] - e^{-(q-\omega)} \left[1 + \frac{1}{8} \left(\frac{1}{\omega} - \frac{1}{q} \right) \right] \right\} \\ B_1(\omega) &\sim \frac{1}{2\sqrt{q\omega}} \left\{ e^{(q-\omega)} \left[1 + \frac{1}{8} \left(\frac{3}{\omega} + \frac{1}{q} \right) \right] + e^{-(q-\omega)} \left[1 - \frac{1}{8} \left(\frac{3}{\omega} + \frac{1}{q} \right) \right] \right\} \end{aligned} \right\} \quad (18a)$$

The last results can now be substituted in the transform equation (17), and the following approximate ($p \rightarrow \infty$) formula is found:

$$\frac{T_C - T_1}{T_0 - T_1} \sim \frac{m}{\sqrt{\rho_0 p}} \left[\frac{e^{-q(p-\rho_0)}}{p(q+\gamma)} - \frac{1}{8} \frac{1-p}{p} \frac{e^{-q(p-\rho_0)}}{pq(q+\gamma)} \right] \quad (19)$$

where

$$\gamma = \frac{1}{8\rho_0} (3 + \rho_0 + 8m)$$

In this approximation, terms in $e^{-2q(1-\rho_0)}$, etc., have been dropped, on the suppositions that for the present problem there will be most interest in the region where $\rho - \rho_0$ is small and that $1 - \rho_0$ is not small. If the latter condition is violated, so that the wall is quite thin, some of the terms neglected here could easily be included. These terms represent the influence of the outer wall. It is an advantage of this expansion method that such influences can be identified and the ones of interest in particular cases examined separately.

The transform in equation (19) can now be inverted; the result is, for small values of τ ,

$$\begin{aligned} \frac{T_C(\rho, \tau) - T_1}{T_0 - T_1} &\doteq \frac{m}{\gamma\sqrt{\rho_0 p}} \left\{ \left[1 + \frac{1-p}{8\rho} \left(\frac{1}{\gamma} + p - \rho_0 \right) \right] \operatorname{erfc} \frac{\rho - \rho_0}{2\sqrt{\tau}} - \frac{1-p}{4\rho} \left(\frac{\tau}{\pi} \right)^{1/2} \exp \left[-\frac{(p-\rho_0)^2}{4\tau} \right] \right. \\ &\quad \left. - \left(1 + \frac{1}{\gamma} \frac{1-p}{8\rho} \right) \exp[\gamma(p - \rho_0) + \gamma^2\tau] \operatorname{erfc} \left(\frac{\rho - \rho_0}{2\sqrt{\tau}} + \gamma\sqrt{\tau} \right) \right\} \end{aligned} \quad (20)$$

It will be noted that equation (19) is not fully expanded in powers of q^{-1} but, rather, the denominator $(q + \gamma)$ is kept intact. In the limit $t \rightarrow 0$, results of the two processes must, of course, coincide, but there is a physical reason for using the expansion as in equation (19) rather than a complete expansion in powers of q^{-1} . In the approximations used above, where the effect of the outer wall is neglected, and if curvature is also neglected, the problem for the hollow cylinder is like the same problem for a semi-infinite slab. The one-dimensional slab problem is expressed by the equations

$$\frac{\partial^2 T}{\partial x^2} = \frac{\partial T}{\partial \tau} ; \quad T(x, 0) = T_1 ; \quad \lim_{x \rightarrow \infty} T(x, \tau) = T_1$$

$$- \left. \frac{\partial T}{\partial x} \right|_{x=0} = m [T_0 - T(0, \tau)]$$

The solution for this problem, in transform notation, is

$$\begin{aligned} \frac{T - T_1}{T_0 - T_1} &= m \frac{e^{-qx}}{p(q + m)} = m \frac{e^{-qx}}{pq} \left(1 + \frac{m}{q}\right)^{-1} \\ &= m \frac{e^{-qx}}{pq} \left(1 - \frac{m}{q} + \frac{m^2}{q^2} - \dots\right) \end{aligned}$$

The partial sums of the last series can be interpreted as successive approximations to the solution of the problem in question. For, if

$$T^{(0)}(x, \tau) = T_1$$

and a sequence of solutions of the diffusion equation is defined by the conditions

$$T^{(i)}(x, 0) = T_1$$

$$\begin{aligned} \lim_{x \rightarrow \infty} T^{(i)}(x, \tau) &= T_1 \\ - \frac{\partial T^{(i)}}{\partial x} &= m [T_0 - T^{(i-1)}(0, \tau)] \end{aligned}$$

then the Laplace transform of the quantity $(T_{(n)}(x, \tau) - T_1)/(T_0 - T_1)$ coincides with the n th partial sum of the series expansion above. Thus, there is introduced by the expansion in powers of q^{-1} an additional approximation in which the boundary condition is never exactly satisfied. This would seem to explain why the results obtained in the original problem by keeping the term $(q + \gamma)^{-1}$ are somewhat better than those found by straightforward expansion in powers of q^{-1} , as will appear below when comparison with machine-computed results is made. For reference purposes, the expansion in terms of q^{-1} is

$$\frac{T_C(\rho, \tau) - T_1}{T_0 - T_1} \doteq \frac{m}{\sqrt{\rho_0 \rho}} \left[2\tau^{1/2} i_{erfc} \frac{\rho - \rho_0}{2\sqrt{\tau}} + \frac{1}{2} \left(\frac{1}{\rho_0} - \frac{1}{\rho} - 4 \frac{1 + 2m}{\rho_0} \right) \tau i^2_{erfc} \frac{\rho - \rho_0}{2\sqrt{\tau}} \right] \quad (20a)$$

The functions $i^n_{erfc} x$ are defined as

$$i^n_{erfc} x = \int_x^\infty i^{n-1}_{erfc} \xi d\xi$$

$$i^0_{erfc} x = erfc x = \frac{2}{\sqrt{\pi}} \int_x^\infty e^{-\xi^2} d\xi$$

Tabulations of this integrated error function can be found in references 16 and 19.

It is found that the results given by the approximate formula (20) are adequate for the smaller values of Biot number m , but when $m > 1$, accuracy falls off. This situation can be remedied by writing

$$\frac{T_C - T_1}{T_0 - T_1} = \frac{T_A - T_1}{T_0 - T_1} + \frac{T_C - T_A}{T_0 - T_1} \quad (20b)$$

and expanding the two terms on the right side separately. The expansion for T_A will be given shortly, and the difference term is approximated by the following expression:

$$\begin{aligned} \frac{T_C - T_A}{T_0 - T_1} \\ \doteq -\sqrt{\frac{\rho_0}{\rho}} \left\{ \left[1 - \frac{1}{8\gamma} \left(\frac{4}{\rho_0} + 1 - \frac{1}{\rho} \right) \right] \exp[\gamma(\rho - \rho_0) + \gamma^2 \tau] i_{erfc} \left(\frac{\rho - \rho_0}{2\sqrt{\tau}} + \kappa\sqrt{\tau} \right) \right. \\ \left. + \frac{1}{8\gamma} \left(\frac{4}{\rho_0} + 1 - \frac{1}{\rho} \right) erfc \frac{\rho - \rho_0}{2\sqrt{\tau}} \right\} \end{aligned} \quad (20c)$$

The small τ results for cases A and B of heat input are

$$\frac{T_A(\rho, \tau) - T_1}{T_0 - T_1} = \sqrt{\frac{\rho_0}{\rho}} \left\{ \left(1 + \frac{1}{d} \frac{1 - \rho}{8\rho} \right) \exp[d(\rho - \rho_0) + d^2\tau] \operatorname{erfc} \left(\frac{\rho - \rho_0}{2\sqrt{\tau}} + d\sqrt{\tau} \right) \right. \\ \left. - \frac{1}{d} \frac{1 - \rho}{8\rho} \operatorname{erfc} \frac{\rho - \rho_0}{2\sqrt{\tau}} \right\} \quad (21)$$

where

$$d = \frac{\rho_0 - 1}{8\rho_0}$$

$$\frac{T_B(\rho, \tau) - T_1}{b/k} = \frac{1}{\beta\sqrt{\rho_0\rho}} \left(\left(1 + \frac{1}{8\beta} \frac{1 - \rho}{\rho} \right) \left\{ \operatorname{erfc} \frac{\rho - \rho_0}{2\sqrt{\tau}} \right. \right. \\ \left. \left. - \exp[\beta(\rho - \rho_0) + \beta^2\tau] \operatorname{erfc} \left(\frac{\rho - \rho_0}{2\sqrt{\tau}} + \beta\sqrt{\tau} \right) \right\} \right. \\ \left. - \frac{1 - \rho}{4\rho} \left(\frac{1}{\pi} \right)^{1/2} \exp \left[- \frac{(\rho - \rho_0)^2}{4\tau} \right] + (\rho - \rho_0) \frac{1 - \rho}{8\rho} \operatorname{erfc} \frac{\rho - \rho_0}{2\sqrt{\tau}} \right) \quad (22)$$

where

$$\beta = \frac{3 + \rho_0}{8\rho_0}$$

Comparisons of the above approximate results with some machine-calculated ones appear in figure 2. The latter are based on the series given in equations (6), (7), and (8). The cases $m = 0, 0.1, 1.0, 10.0, \infty$ are shown with $\rho_0 = 0.15$.

It should be mentioned that the quantity plotted as V_C differs according as $m < 1$ or > 1 . For $m > 1$,

$$V_C = \frac{T_C - T_1}{T_0 - T_1}$$

and as $m \rightarrow \infty$

$$\lim_{m \rightarrow \infty} V_C = V_A$$

which can be verified by comparison of equations (6) and (7). On the other hand, for small m ,

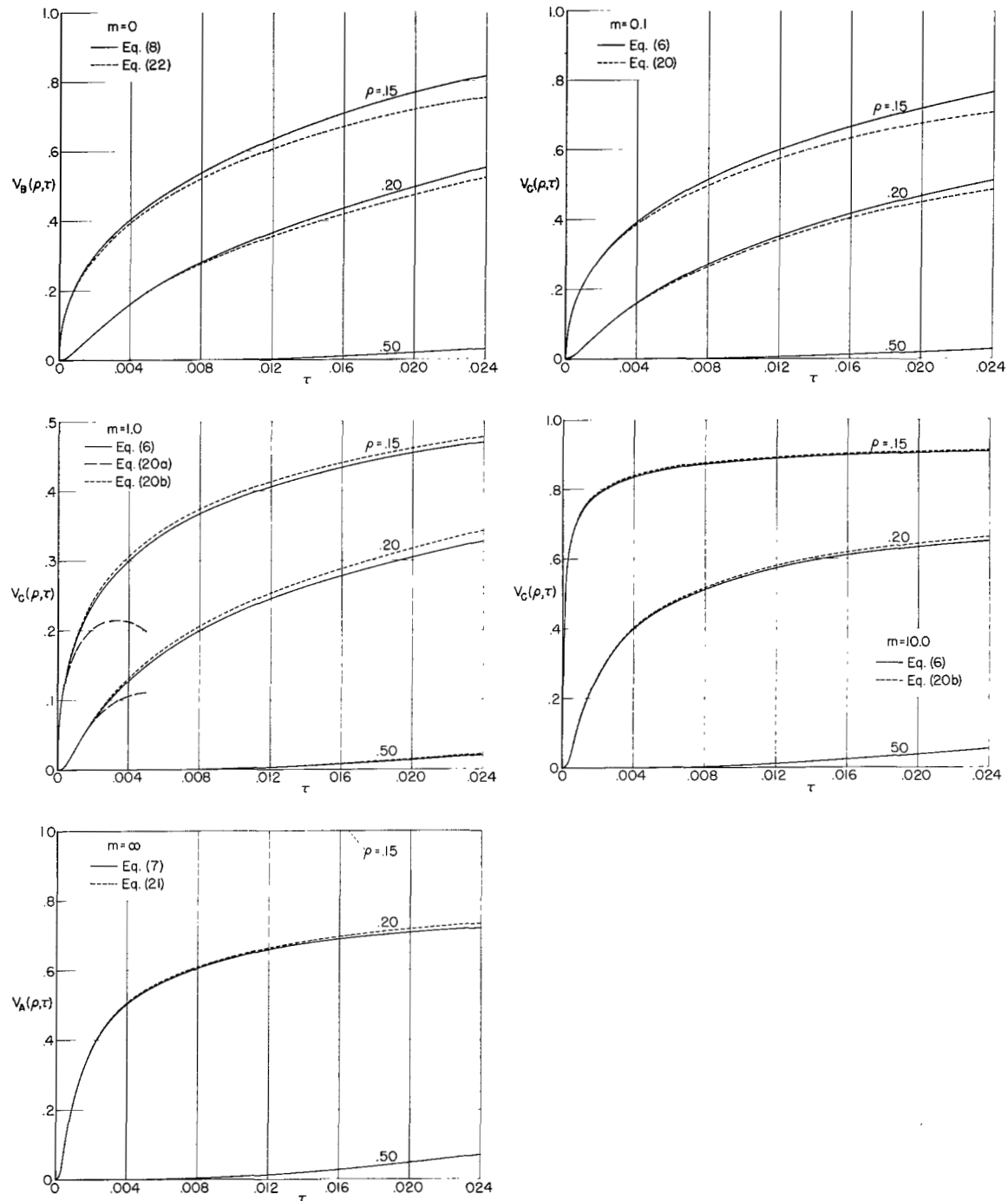


Figure 2.- Comparison of exact and approximate (small τ) results for temperature.

$$\lim_{m \rightarrow 0} \frac{T_C - T_1}{m(T_O - T_1)} = \frac{T_B - T_1}{b/k}$$

as discussed at equation (8). The quantity V_C is thus defined as

$$V_C = \frac{1}{m} \frac{T_C - T_1}{T_O - T_1}$$

when $m < 1$, so that there is a smooth approach to the limit as $m \rightarrow 0$. Note that the temperature ratio $(T_C - T_1)/(T_O - T_1)$ for $m < 1$ is obtained by multiplying the shown quantity V_C by m . This does not hold in the limit $m = 0$, where the quantity graphed is

$$V_B = \frac{T_B - T_1}{b/k}$$

since the temperature analogous to the ambient T_O is then undefined. Curves are drawn for values of ρ generally near the inner boundary, which is the region of greatest interest at small times. The agreement between the approximate and exact results is seen to be quite good up to about $\tau = 0.01$, but the approximate results become more and more in error thereafter.

Also shown, on the portion of figure 2 corresponding to $m = 1.0$, are the asymptotic results from an expansion in powers of q^{-1} (eq. (20a)). These are seen to be much worse than the ones actually used, which prompted the remarks above on choice of expansion for the temperature.

Although not shown, a few calculations for a disk with a thinner wall ($\rho_O = 0.5$) indicate that agreement between exact and approximate results for small τ is even better than for $\rho_O = 0.15$. A concomitant which must be accepted is that these results will become less adequate for thicker walls, that is, for $\rho_O < 0.15$ say. If the error becomes unacceptable for such small ρ_O , it may prove profitable to use Goldstein's device (ref. 15) in which functions of $(q\rho_O)$ are expanded for small rather than for large argument.

Approximation for the integral $I(\rho, \rho_O; \tau)$. - The integral defined in equation (10d) must be calculated before the displacement and stresses can be found. Using the form (17) for the temperature, it is found that

$$\begin{aligned} \overline{I_C(\rho, \rho_O; \tau)} &= \frac{m}{p} [mB_O(q\rho_O) - q\rho_O B_1(q\rho_O)]^{-1} \int_{\rho_O}^{\rho} \rho_1 B_O(q\rho_1) d\rho_1 \\ &= \frac{m}{pq} \frac{\rho B_1(q\rho) - \rho_O B_1(q\rho_O)}{mB_O(q\rho_O) - q\rho_O B_1(q\rho_O)} \end{aligned} \quad (23)$$

Straightforward expansion using the asymptotic formulae (18a) gives

$$\begin{aligned} \overline{I_C(\rho, \rho_0; p)} &\sim \frac{m}{pq(q + \gamma)} \left[1 - \sqrt{\frac{\rho}{\rho_0}} e^{-q(\rho - \rho_0)} \right] \\ &+ \frac{m}{8p^2(q + \gamma)} \left[1 + \frac{3}{\rho_0} - \left(1 + \frac{3}{\rho} \right) \sqrt{\frac{\rho}{\rho_0}} e^{-q(\rho - \rho_0)} \right] \end{aligned} \quad (24a)$$

where again

$$\gamma = \frac{1}{8\rho_0} (3 + \rho_0 + 8m)$$

This result can be inverted to yield

$$\begin{aligned} I_C(\rho, \rho_0; \tau) &\doteq m \left\{ \frac{1}{\gamma^2} \left[-1 + 2\gamma \left(\frac{\tau}{\pi} \right)^{1/2} + e^{\gamma^2 \tau} \operatorname{erfc}(\gamma\sqrt{\tau}) \right] \left[1 - \frac{1}{8\gamma} \left(1 + \frac{3}{\rho_0} \right) \right] + \frac{\tau}{8\gamma} \left(1 + \frac{3}{\rho_0} \right) \right\} \\ &- m \sqrt{\frac{\rho}{\rho_0}} \left(\frac{1}{\gamma^2} \left[1 - \frac{1}{8\gamma} \left(1 + \frac{3}{\rho} \right) \right] \left\{ -\operatorname{erfc} \frac{\rho - \rho_0}{2\sqrt{\tau}} + 2\gamma\sqrt{\tau} \operatorname{i erfc} \frac{\rho - \rho_0}{2\sqrt{\tau}} \right. \right. \\ &\left. \left. + \exp[\gamma(\rho - \rho_0) + \gamma^2 \tau] \operatorname{erfc} \left(\frac{\rho - \rho_0}{2\sqrt{\tau}} + \gamma\sqrt{\tau} \right) \right\} + \frac{1}{8\gamma} \left(1 + \frac{3}{\rho} \right) 4\tau i^2 \operatorname{erfc} \frac{\rho - \rho_0}{2\sqrt{\tau}} \right) \end{aligned} \quad (24b)$$

The result in equation (24b) is adequate for the smaller values of the parameter m shown in figure 3, but the accuracy is falling off as m increases. It is possible to improve the approximation somewhat for larger values of m by the same device that was used above for the temperature:

$$I_C = I_A + (I_C - I_A) \quad (25)$$

and expanding the difference expression separately. The expansion of I_A for small τ will be given later. The difference expression is, for large q ,

$$\begin{aligned} \overline{I_C - I_A} &= \frac{1}{pq} \frac{q\rho_0 B_1(q\rho_0)}{B_0(q\rho_0)} \frac{\rho B_1(q\rho) - \rho_0 B_1(q\rho_0)}{m B_0(q\rho_0) - q\rho_0 B_1(q\rho_0)} \\ &\sim \frac{\rho_0}{p(q + \gamma)} \left\{ \sqrt{\frac{\rho}{\rho_0}} \left[1 + \frac{1}{8q} \left(1 + \frac{3}{\rho} + \frac{4}{\rho_0} \right) e^{-q(\rho - \rho_0)} \right] - 1 - \frac{1}{8q} \left(\frac{7}{\rho_0} + 1 \right) \right\} \end{aligned} \quad (25a)$$

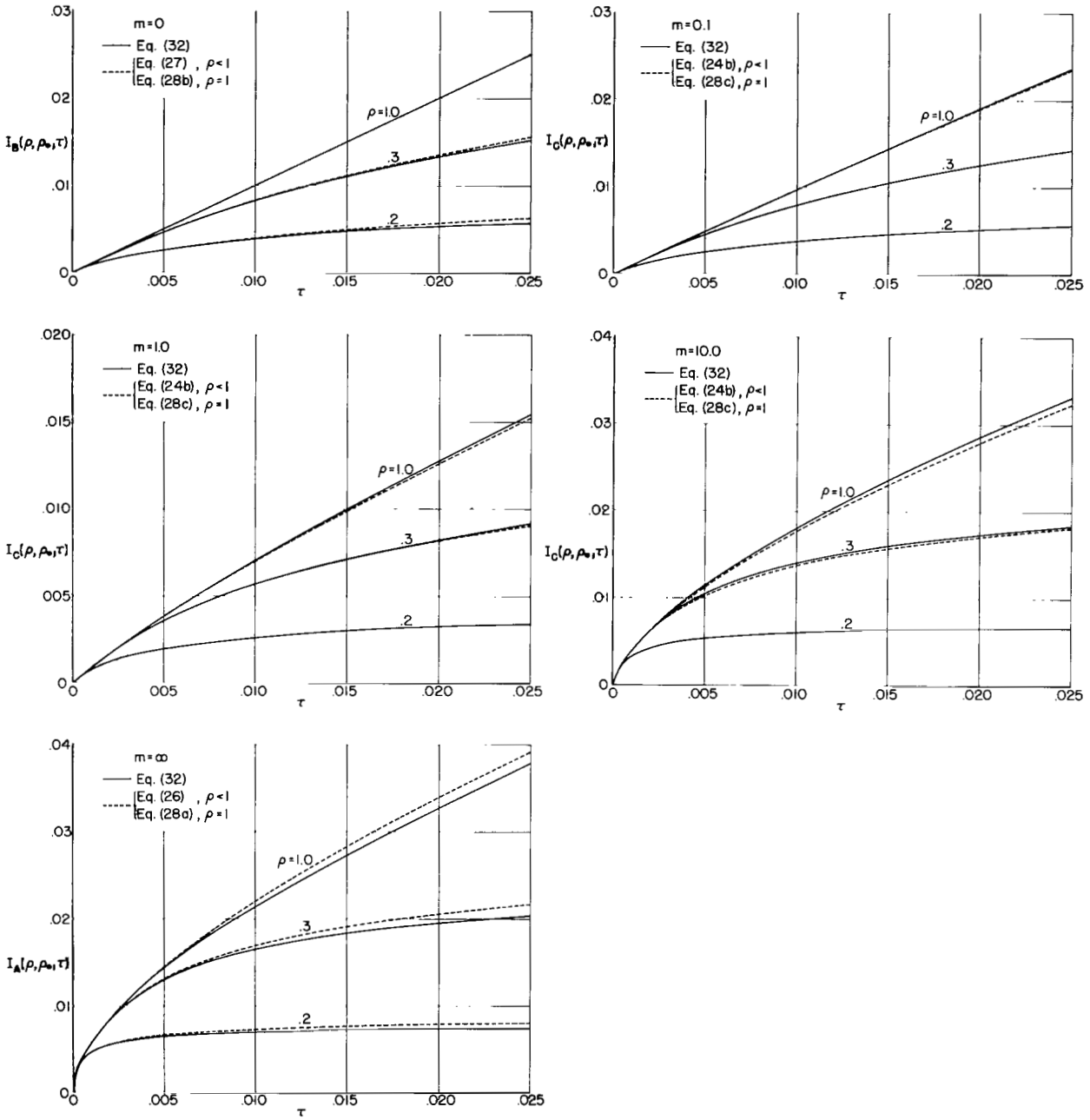


Figure 3.- Comparison of exact and approximate (small τ) results for the integral $I(p, \rho_0; \tau)$.

The last expression can be inverted to give, for small τ :

$$\begin{aligned}
 I_C - I_A &\doteq p_0 \left(\frac{1}{\gamma} \sqrt{\frac{p}{p_0}} \left\{ \operatorname{erfc} \frac{p - p_0}{2\sqrt{\tau}} - \exp[\gamma(p - p_0) + \gamma^2 \tau] \operatorname{erfc} \left(\frac{p - p_0}{2\sqrt{\tau}} + \gamma\sqrt{\tau} \right) \right\} \right. \\
 &+ \frac{1}{8\gamma^2} \sqrt{\frac{p}{p_0}} \left(1 + \frac{3}{p} + \frac{4}{p_0} \right) \left\{ \exp[\gamma(p - p_0) + \gamma^2 \tau] \operatorname{erfc} \left(\frac{p - p_0}{2\sqrt{\tau}} + \gamma\sqrt{\tau} \right) \right. \\
 &- \left. \operatorname{erfc} \frac{p - p_0}{2\sqrt{\tau}} + 2\gamma\sqrt{\tau} i \operatorname{erfc} \frac{p - p_0}{2\sqrt{\tau}} \right\} - \frac{1}{\gamma} \left[1 - e^{\gamma^2 \tau} \operatorname{erfc}(\gamma\sqrt{\tau}) \right] \\
 &\left. - \frac{1}{8\gamma^2} \left(\frac{7}{p_0} + 1 \right) \left[e^{\gamma^2 \tau} \operatorname{erfc}(\gamma\sqrt{\tau}) - 1 + 2\gamma \left(\frac{\tau}{\pi} \right)^{1/2} \right] \right) \quad (25b)
 \end{aligned}$$

In order to use this expression in the calculation of I_C , it is necessary to have the small τ expansion for I_A . This is given below, together with that for I_B .

$$\begin{aligned}
 I_A(p, p_0; \tau) &\doteq p_0 \left\{ 2 \left(\frac{\tau}{\pi} \right)^{1/2} + \frac{\tau}{2p_0} - \sqrt{\frac{p}{p_0}} \left[2\tau^{1/2} i \operatorname{erfc} \frac{p - p_0}{2\sqrt{\tau}} \right. \right. \\
 &\left. \left. + \frac{1}{2} \left(\frac{1}{p_0} + \frac{3}{p} \right) \tau i^2 \operatorname{erfc} \frac{p - p_0}{2\sqrt{\tau}} \right] \right\} \quad (26)
 \end{aligned}$$

$$I_B(p, p_0; \tau) \doteq \tau - \sqrt{\frac{p}{p_0}} \left[4\tau i^2 \operatorname{erfc} \frac{p - p_0}{2\sqrt{\tau}} - 3 \left(\frac{1}{p_0} - \frac{1}{p} \right) \tau^{3/2} i^3 \operatorname{erfc} \frac{p - p_0}{2\sqrt{\tau}} \right] \quad (27)$$

Finally, it is necessary to know the values taken by the integral $I(p, p_0; \tau)$ when $p = 1$. That it is not strictly correct simply to put $p = 1$ in the foregoing approximate expressions is obvious because the terms in $e^{-q(1-p)}$ were eliminated on the basis that p is not close to unity. Thus, by the Wronskian of $I_0(z)$, $K_0(z)$

$$B_1(q) = q^{-1}$$

while the approximation (18a) gives, when the negative exponential is neglected,

$$B_1(q) \sim \frac{1}{2q} \left(1 + \frac{1}{2q} \right)$$

Thus, by putting $\rho = 1$ before using the asymptotic expressions, it is found that

$$I_A(1, \rho_0; \tau) \doteq \rho_0 \left\{ 2 \left(\frac{\tau}{\pi} \right)^{1/2} + \frac{\tau}{2\rho_0} - \frac{2}{\sqrt{\rho_0}} \left[2\tau^{1/2} \operatorname{erfc} \frac{1 - \rho_0}{2\sqrt{\tau}} \right. \right. \\ \left. \left. + 2 \left(\frac{1}{\rho_0} - 1 \right) \tau^{1/2} \operatorname{erfc} \frac{1 - \rho_0}{2\sqrt{\tau}} \right] \right\} \quad (28a)$$

$$I_B(1, \rho_0; \tau) \doteq \tau - \frac{2}{\sqrt{\rho_0}} \left[4\tau^{1/2} \operatorname{erfc} \frac{1 - \rho_0}{2\sqrt{\tau}} - \left(\frac{3}{\rho_0} + 1 \right) \tau^{3/2} i^{3/2} \operatorname{erfc} \frac{1 - \rho_0}{2\sqrt{\tau}} \right] \\ (28b)$$

$$I_C(1, \rho_0; \tau) \doteq m \left\{ \frac{1}{\gamma^2} \left[1 - \frac{1}{8\gamma} \left(\frac{3}{\rho_0} + 1 \right) \right] \left[e^{\gamma^2 \tau} \operatorname{erfc} \left(\gamma \tau^{1/2} \right) - 1 + 2\gamma \left(\frac{\tau}{\pi} \right)^{1/2} \right] \right. \\ \left. + \frac{1}{8\gamma} \left(\frac{3}{\rho_0} + 1 \right) \tau \right\} - \frac{2m}{\gamma^2 \rho_0^{1/2}} \left[e^{\gamma(1-\rho_0)+\gamma^2 \tau} \operatorname{erfc} \left(\frac{1 - \rho_0}{2\tau^{1/2}} + \gamma \tau^{1/2} \right) \right. \\ \left. - \operatorname{erfc} \frac{1 - \rho_0}{2\tau^{1/2}} + 2\gamma \tau^{1/2} i \operatorname{erfc} \frac{1 - \rho_0}{2\tau^{1/2}} \right] \quad (28c)$$

$$I_C - I_A|_{\rho=1} \doteq - \frac{\rho_0}{\gamma} \left[1 - \frac{1}{8\gamma} \left(\frac{7}{\rho_0} + 1 \right) \right] \left(1 - e^{-\gamma^2 \tau} \operatorname{erfc} \gamma \sqrt{\tau} \right) - \frac{\rho_0}{4\gamma} \left(\frac{7}{\rho_0} + 1 \right) \left(\frac{\tau}{\pi} \right)^{1/2} \\ + 2 \frac{\sqrt{\rho_0}}{\gamma} \left(1 - \frac{1}{2\gamma \rho_0} \right) \left[e^{\gamma(1-\rho_0)+\gamma^2 \tau} \operatorname{erfc} \left(\frac{1 - \rho_0}{2\sqrt{\tau}} + \gamma \sqrt{\tau} \right) - \operatorname{erfc} \frac{1 - \rho_0}{2\sqrt{\tau}} \right] \\ - \frac{2}{\gamma \sqrt{\rho_0}} \sqrt{\tau} i \operatorname{erfc} \frac{1 - \rho_0}{2\sqrt{\tau}} \quad (28d)$$

Figure 3 shows comparison of exact and approximate results for the integral $I(\rho, \rho_0; \tau)$. They appear to be of better reliability than those shown earlier for the temperature, probably because they represent integrated quantities. The same convention on multiplication by Biot number m applies here as for the temperatures in figure 2.

CALCULATION OF TEMPERATURE AND STRESSES

The calculations amount essentially to summing the series derived in previous sections, such as equation (6), and determining the integral $I(\rho, \rho_0; \tau)$

(see eq. (10d)). A series expansion of this integral will be given below. Although the series are convergent, the favorable damping due to the factor $e^{-\mu n^2 \tau}$ in each term is somewhat delayed when τ is small, say $\tau < 10^{-2}$. In this event it is sometimes necessary to consider upwards of 30 terms of the series in order to achieve four significant figures. Fortunately, the terms alternate in sign so the maximum error (and its sign) caused by stopping at a given term is known.

Calculation of Eigenvalues

Determination of the sums indicated in equations (6), (7), (8) and of the integral in (10d) requires that the eigenvalues $\mu_n(\alpha_n, \beta_n)$ be found. These are defined by equation (6a) ((7a), (8a)). It is possible to derive approximate expressions for the eigenvalues when n is large by making use of the asymptotic expressions for the Bessel functions (see ref. 17). Denote, for large values of the argument,

$$\left. \begin{aligned} J_0(x) &\sim \left(\frac{2}{\pi x}\right)^{1/2} [P_0(x)\cos x_1 - Q_0(x)\sin x_1] \\ J_1(x) &\sim \left(\frac{2}{\pi x}\right)^{1/2} [P_1(x)\sin x_1 + Q_1(x)\cos x_1] \\ Y_0(x) &\sim \left(\frac{2}{\pi x}\right)^{1/2} [P_0(x)\sin x_1 + Q_0(x)\cos x_1] \\ Y_1(x) &\sim \left(\frac{2}{\pi x}\right)^{1/2} [-P_1(x)\cos x_1 + Q_1(x)\sin x_1] \end{aligned} \right\} \quad (29)$$

where

$$P_j(x) = \sum_{m=0}^{\infty} \frac{(-1)^m (j, 2m)}{(2x)^{2m}}$$

$$Q_j(x) = \sum_{m=0}^{\infty} \frac{(-1)^m (j, 2m+1)}{(2x)^{2m+1}}$$

$$(j, k) = \frac{1}{2^{2k} k!} \left\{ (4j^2 - 1^2)(4j^2 - 3^2) \dots [4j^2 - (2k-1)^2] \right\}$$

and

$$x_1 = x - \frac{\pi}{4}$$

These expressions are now to be inserted in equation (6a). The result is

$$\tan(1 - \rho_0)x = \frac{m[P_0(x)Q_0(\rho_0x) - P_0(\rho_0x)Q_0(x)] - \rho_0x[P_1(x)P_1(\rho_0x) + Q_0(x)Q_1(\rho_0x)]}{m[P_0(x)P_0(\rho_0x) + Q_0(x)Q_0(\rho_0x)] + \rho_0x[P_0(x)Q_1(\rho_0x) - P_1(\rho_0x)Q_0(x)]} \quad (30)$$

where x now stands for the eigenvalues μ_n . To solve for those eigenvalues, a process of successive approximation can be used, starting by neglecting all but lowest powers of x^{-1} in the expression on the right. For example, in the first approximation

$$\tan(1 - \rho_0)x \sim -\frac{x}{\gamma}$$

This relation shows the characteristic behavior of the well-known transcendental equation

$$\tan x = -x$$

That is, the n th root approaches $[n - (1/2)]\pi$ as n increases. In the present case, the first approximation to the eigenvalue μ_n for large n is

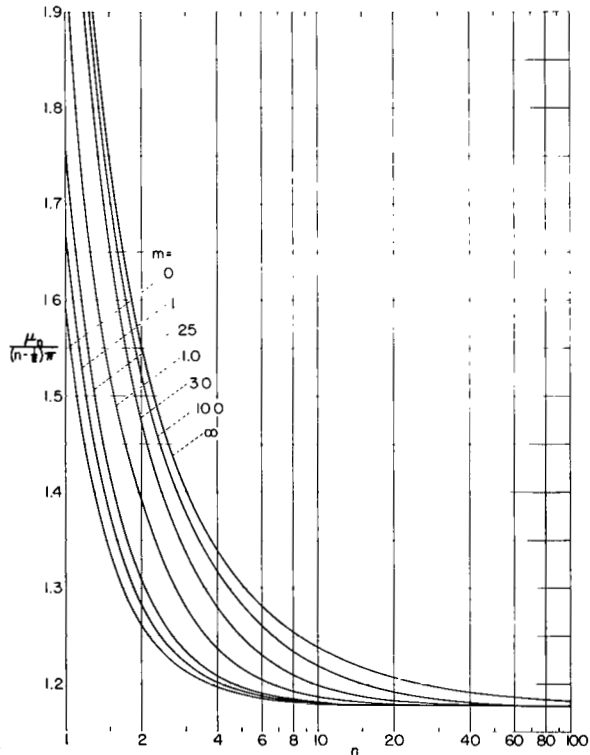


Figure 4.- Variation of the eigenvalues μ_n with n , and with Biot number m (eq. (6a), $\rho_0 = 0.15$).

$$\mu_n \sim \frac{\left(n - \frac{1}{2}\right)\pi}{1 - \rho_0} + \frac{\gamma}{\left(n - \frac{1}{2}\right)\pi} \quad (31)$$

Further approximations can be obtained if desired, if the result (31) is substituted into equation (30) and terms involving higher powers of $\{[n - (1/2)]\pi\}^{-1}$ are determined.

Such approximations were not used (except for checking purposes) in the present calculations. It was found as easy to use the complete frequency equation (6a) and determine the roots by means of a simple interpolatory procedure. A standard program for Bessel functions was used when the argument $x \leq 20$, and extensions made by use of the asymptotic formulae (29). Figure 4 shows the variation of the eigenvalues (actually $\mu_n/[n - (1/2)\pi]$) with n ,

and also with the Biot number m which appears as a parameter in the frequency equation. Limiting values $m \rightarrow \infty$ where $\mu_n \rightarrow \alpha_n$ and $m = 0$ where $\mu_n = \beta_n$ are shown. The eigenvalues for $m = 100, 0.01$ are nearly indistinguishable from those for $m \rightarrow \infty, 0$, respectively. This particular graph is drawn for $\rho_0 = 0.15$, so the limiting value as $n \rightarrow \infty$ is

$$\lim_{n \rightarrow \infty} \frac{\mu_n}{\left(n - \frac{1}{2}\right)\pi} = \frac{1}{1 - \rho_0} = 1.18 \dots$$

Summation of Series Expressions

Once the eigenvalues are known, one can continue with the summation process. In this, it was found adequate, for $\tau \geq 5 \times 10^{-4}$, to provide for using, at most, 50 terms of the series. The computation halted automatically at a value of n such that the corresponding term was less in absolute magnitude than 1×10^{-7} .

The integral $I(\rho, \rho_0; \tau)$ defined in equation (10d) can also be expressed as an infinite series. Using equation (6) for temperature, it is found that

$$\begin{aligned} I_C(\rho, \rho_0; \tau) &= \frac{m}{1 + m \log\left(\frac{1}{\rho_0}\right)} \left[\frac{\rho^2 - \rho_0^2}{4} + \frac{1}{2} \left(\rho^2 \log \frac{1}{\rho} - \rho_0^2 \log \frac{1}{\rho_0} \right) \right] \\ &- 2m^2 \sum_{n=1}^{\infty} \frac{e^{-\mu_n^2 \tau}}{\mu_n^2} \frac{J_0^2(\mu_n)}{[mJ_0(\rho_0 \mu_n) + \rho_0 \mu_n J_1(\rho_0 \mu_n)]^2 - (m^2 + \rho_0^2 \mu_n^2) J_0^2(\mu_n)} \\ &+ \pi m \rho \sum_{n=1}^{\infty} \frac{e^{-\mu_n^2 \tau}}{\mu_n} \frac{J_0(\mu_n) [mJ_0(\rho_0 \mu_n) + \rho_0 \mu_n J_1(\rho_0 \mu_n)] [J_1(\rho \mu_n) Y_0(\mu_n) - Y_1(\rho \mu_n) J_0(\mu_n)]}{[mJ_0(\rho_0 \mu_n) + \rho_0 \mu_n J_1(\rho_0 \mu_n)]^2 - (m^2 + \rho_0^2 \mu_n^2) J_0^2(\mu_n)} \end{aligned} \quad (32)$$

The results for cases A and B can be obtained from equation (32) by suitable limiting processes performed on m . Results of the calculations outlined above will be presented in the next section.

RESULTS OF COMPUTATIONS

There are an enormous number of possibilities for calculating the stresses, even though the parameters $E, \alpha(\Delta T), a, k$ appear in dimensionless

ratios. A selection from the remaining ones, m , ν , ρ_o , was made which was thought to give a representative selection of cases for different regimes. It is hoped that the cases detailed here will enable one to obtain at least a qualitative notion of the magnitudes and distributions of temperatures, stresses, or displacements in a wide variety of situations. There are available also the fairly simple results for the steady-state values and for the initial variations derived above. These formulae are of course quite general insofar as assigning the parameters m , ν , ρ_o is concerned.

Effect of Variation of Biot Number m

Free outer boundary. - The first case examined is for a fixed geometry ($\rho_o = 0.15$) and Poisson's ratio ($\nu = 0.25$), with the Biot number m allowed to vary between its extremes of 0 and ∞ . All quantities of interest are shown in figures 5 through 9, including curves of the integral $I(\rho, \rho_o; \tau)$ (see eqs. (10d) and (32)). The curves are drawn so that the variation of each quantity with ρ is shown for values of τ covering the range $0.0005 \leq \tau \leq 2$. The latter value of τ is one for which the system has essentially reached its steady state, as indicated by the near identity of the calculations for $\tau = 1$ and $\tau = 2$. The integral $I(\rho, \rho_o; \tau)$ is shown so that the present calculations can easily be extended to stress boundary conditions other than the vanishing of radial stress at $\rho = \rho_o$ and $\rho = 1$. (Some results for the boundary condition of a rigid outer wall will be shown later.) Also, the internal pressure p_o is zero in the calculations for the stresses and displacement; its effect may be included by use of equations (11) or (12).

The values of m for which results are shown are $m = 0(.01)$, 0.1, 1, 10, $\infty(100)$. The numbers in parentheses indicate that the corresponding results differ so little from the results for $m = 0$ and $m \rightarrow \infty$ that they are plotted on the same graph, insofar as they are distinguishable. As discussed above, a difference exists in the dimensionless groups representing temperature, displacement, and stress according as $m < 1$ or $m > 1$. For $m < 1$, m is included in the denominators in order that the dimensionless quantities V_C approach the proper values at $m \rightarrow 0$, corresponding to the constant flux case. For $m > 1$, m is not included in the dimensionless groups so that the proper limits result as $m \rightarrow \infty$, corresponding to the case of sudden change of temperature at $\rho = \rho_o$. Thus, for example,

$$V_C = m^{-1} \frac{T_C - T_1}{T_o - T_1} \quad \text{for } m \leq 1$$

$$= \frac{T_C - T_1}{T_o - T_1} \quad \text{for } m \geq 1$$

This also applies to $I(\rho, \rho_o; \tau)$.

The graphs of the radial temperature distributions show characteristic behavior; the temperature at first rises quickly in a thin layer of material at the inner surface, and the temperature gradient across this layer increases

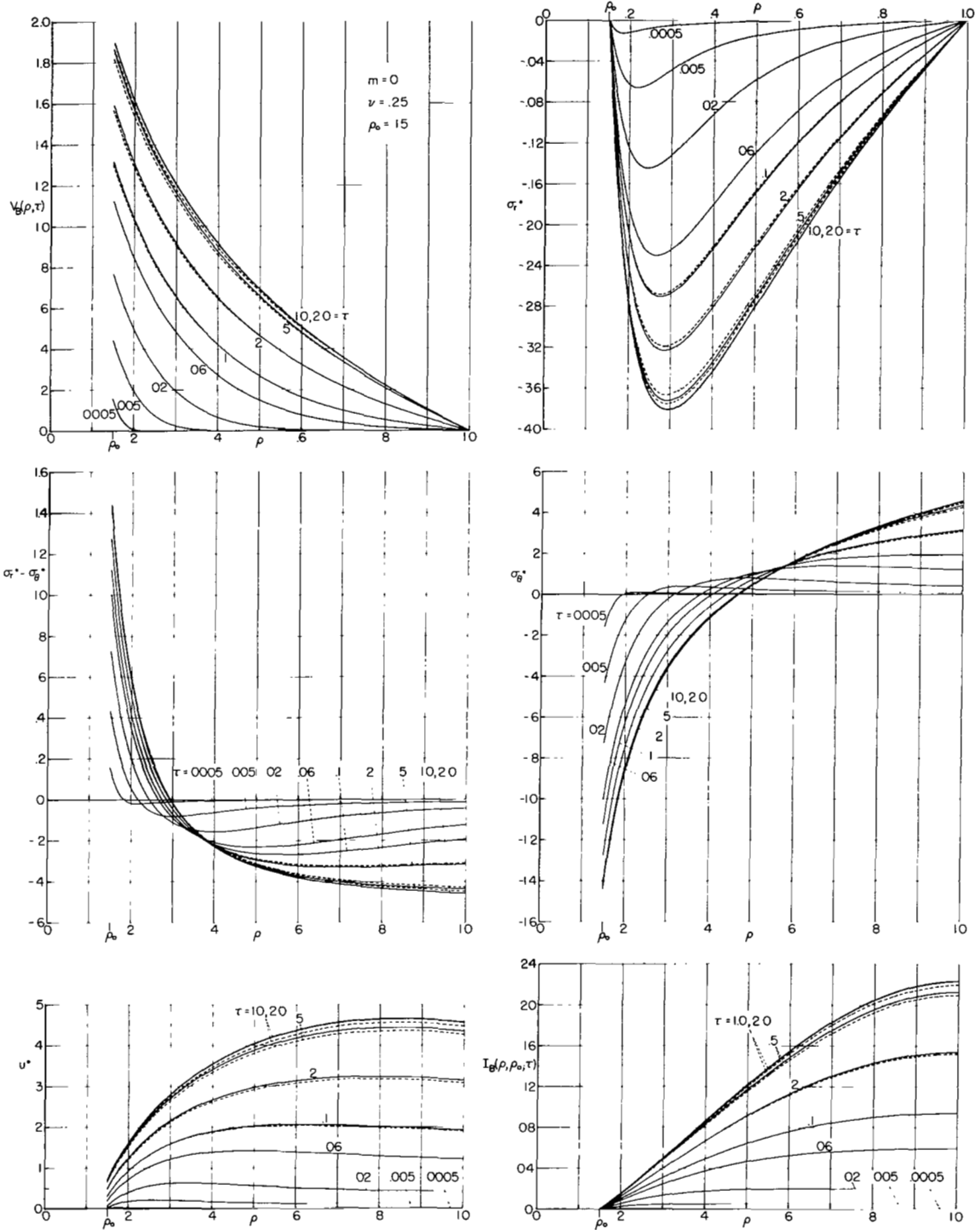


Figure 5.- Transient temperature and stresses for the internally heated disk. Case B; zero stress at $\rho = \rho_0$ and $\rho = 1$.

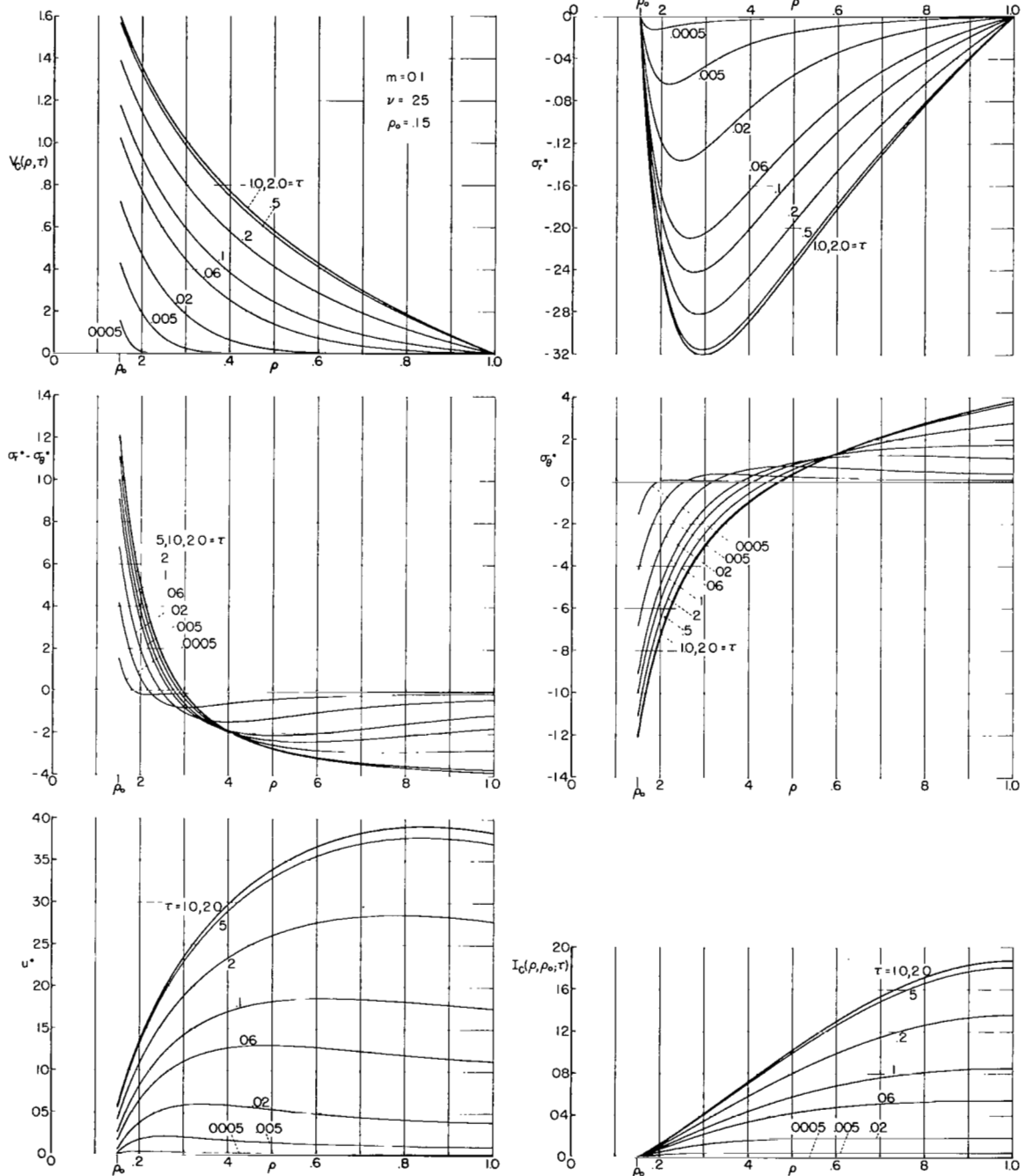


Figure 6.- Transient temperature and stresses for the internally heated disk. Case C ($m = 0.1$); zero stress at $\rho = \rho_0$ and $\rho = 1$.

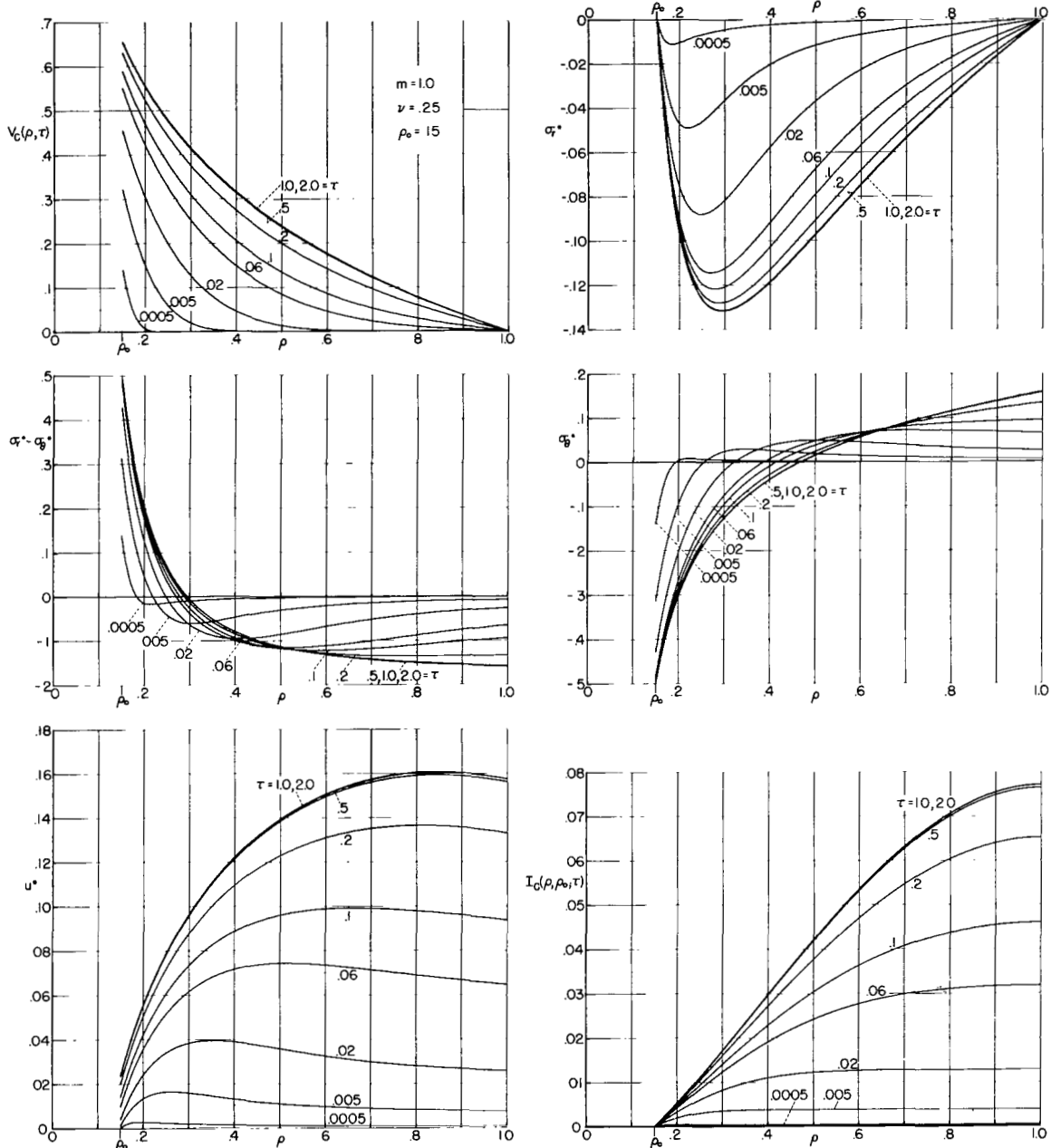


Figure 7-- Transient temperature and stresses for the internally heated disk. Case C ($m = 1.0$); zero stress at $\rho = \rho_0$ and $\rho = 1$.

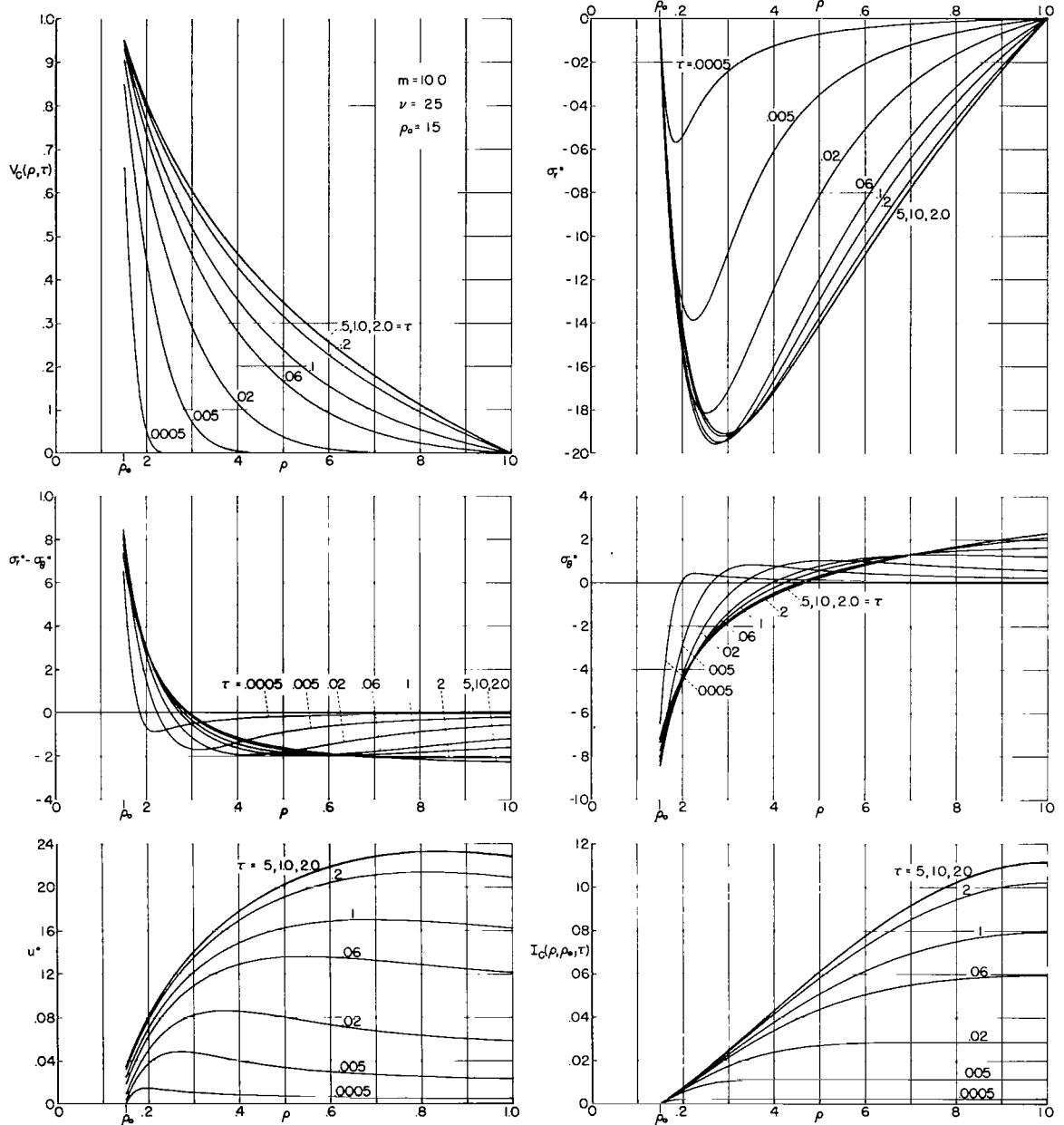


Figure 8.- Transient temperature and stresses for the internally heated disk. Case C ($m = 10.0$); zero stress at $\rho = \rho_0$ and $\rho = 1$.

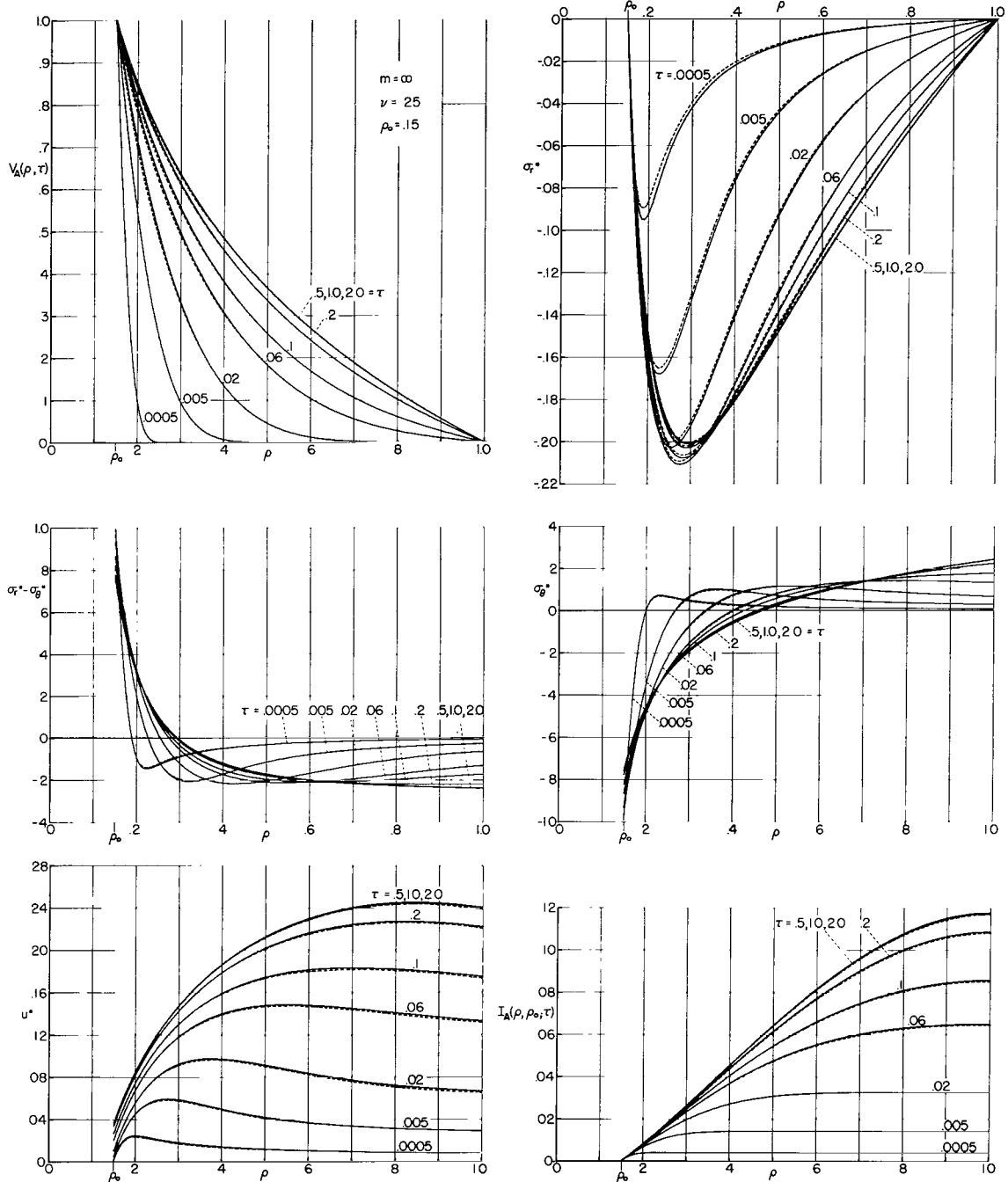


Figure 9.- Transient temperature and stresses for the internally heated disk. Case A; zero stress at $\rho = \rho_0$ and $\rho = l$.

with m . The curves of displacement show, for all values of m , a rather weak maximum at an interior point which moves toward the outer boundary as time increases. The radial stress, which is here zero at both boundaries because $\rho_0 = 0$, shows similar behavior, although the extremum is much accentuated as τ increases. It is, for $T_0 > T_1$, compressive throughout, and its position of numerical maximum moves from the inner wall for $\tau \ll 1$ toward the value $\rho = \rho_{cr}$ predicted in the section on steady-state behavior (eq. (15a)).

In the case of the circumferential stress, a flat extremum occurs at first near the inner boundary, moving to and past the outer boundary as time increases. The value at $\rho = \rho_0$ is the largest compressive stress, and the largest tensile stress occurs eventually at $\rho = 1$. The maximum compressive stress is larger in magnitude than the largest tensile stress, and also larger by a factor of 3 to 5 (depending on m) than the maximum radial compressive stress. The behavior of the circumferential stress distribution is in some respects similar to that of the temperature distribution for small values of τ . That is, it is nonvanishing only in a thin layer near the inner surface, the magnitude at the inner surface and the thickness of the layer increasing with time. For the more intense heating ($m > 1$) the maximum compressive circumferential stress, at $\rho = \rho_0$, no longer occurs in the steady state as it does for the $m \leq 1$ cases. This behavior carries over into the stress difference $(\sigma_r^* - \sigma_\theta^*)$, and figure 10 shows this maximum value as a function of time

for the values $m = 1, 10, \infty$. The curve for $m = 1$ is characteristic of those for the smaller values of m also.

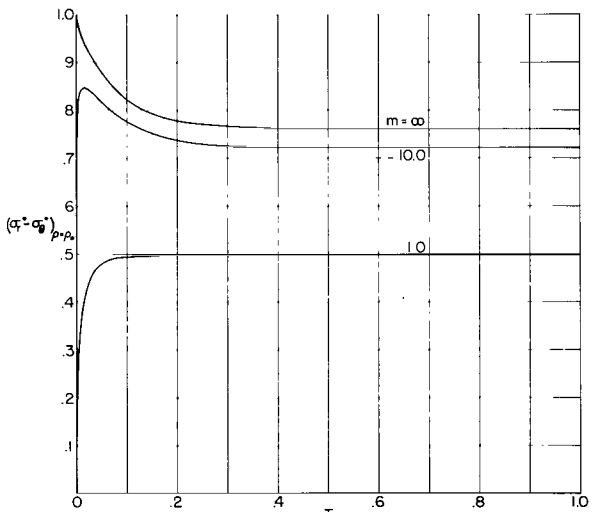
Finally, in figures 5 through 9, the stress difference $(\sigma_r^* - \sigma_\theta^*)$ gives a measure of the maximum shearing stress to be found at any point. At the boundaries, this quantity is dominated by the circumferential stress, and it falls to zero and changes sign somewhat closer to the inner boundary than does σ_θ^* .

Rigidly restrained outer boundary-

In order to gain some notion of the effect of a rigid outer boundary, a few curves will be given in which the results for a free boundary and a fixed boundary are compared. These are drawn only for $m = 0, 1, \infty$ and for values

of τ which show the starting behavior for several values of m ($\rho_0 = 0.15$, $\nu = 0.25$).

and steady state as well as the transitional interval. Also, only the displacement and stress difference are shown. Figure 11, where the displacements for the three values of m are given, shows that initially ($\tau = 0.005$), the differences between the displacements in the cases of zero and complete restraint are rather small. However, as time goes on, the differences increase and, as expected, the free displacements are ultimately considerably greater throughout than those for a rigid restraint. These



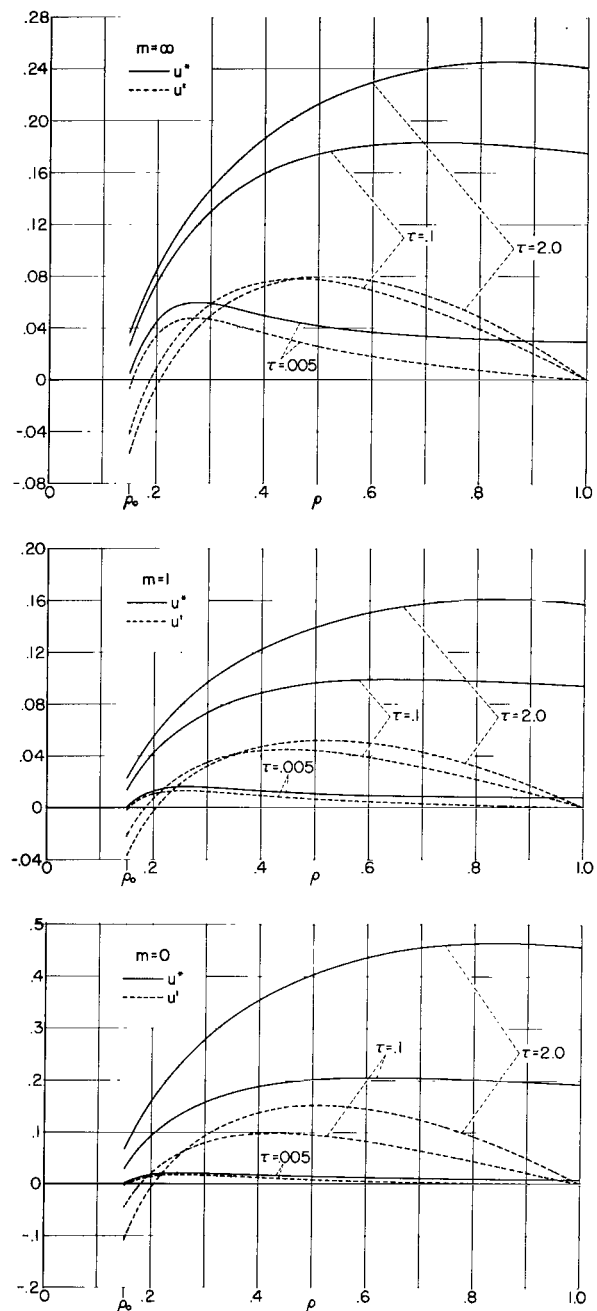


Figure 11.- Comparison of displacements u^* and u' for free and fixed outer boundary, respectively ($\rho_0 = 0.15$, $\nu = 0.25$).

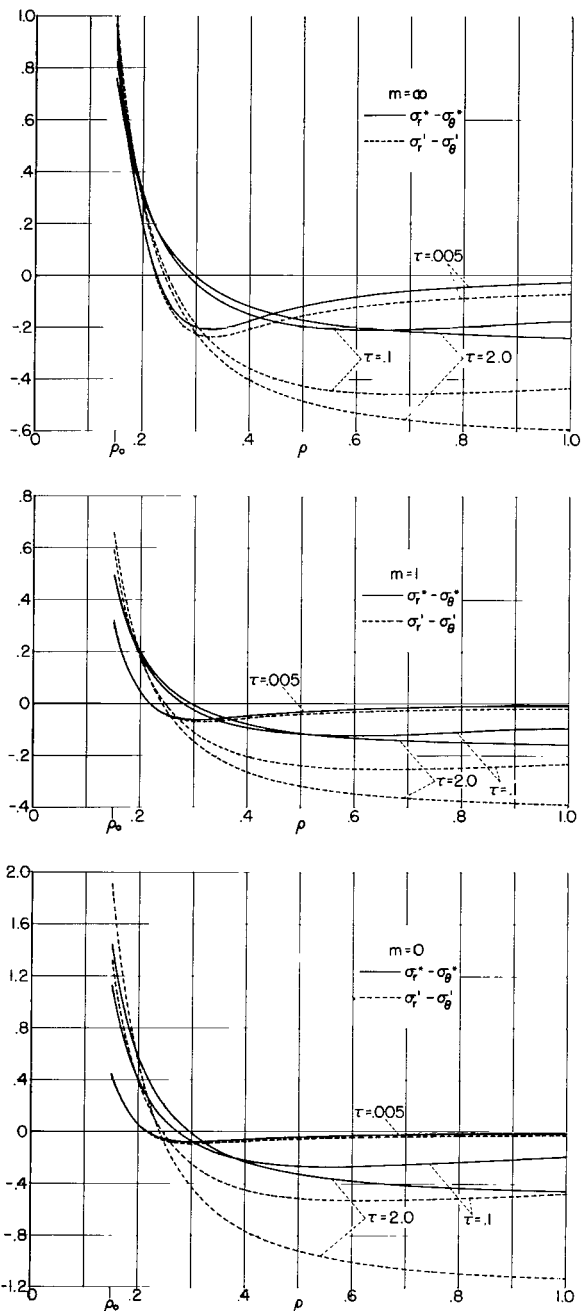


Figure 12.- Comparison of maximum shearing stresses $(\sigma_r^* - \sigma_\theta^*)$ and $(\sigma_r' - \sigma_\theta')$ for free and fixed outer boundary, respectively ($\rho = 0.15$, $\nu = 0.25$).

effects increase in magnitude with the intensity of heating, as would also be expected.

Figure 12 illustrates the differences between the values of $(\sigma_r' - \sigma_\theta')$ and $(\sigma_r^* - \sigma_\theta^*)$, corresponding to fixed and free outer boundaries, respectively. The variation is seen to be similar over the range $\rho_0 < \rho < 1$, the fixed boundary giving the higher magnitudes. Again, differences are heightened by increasing τ and by intensification of heating, or increasing the Biot number m .

Effect of Poisson's Ratio ν

In the free-boundary case, only the displacement u^* is affected by a change of Poisson's ratio. Figure 13 shows the magnitude of the effect for the

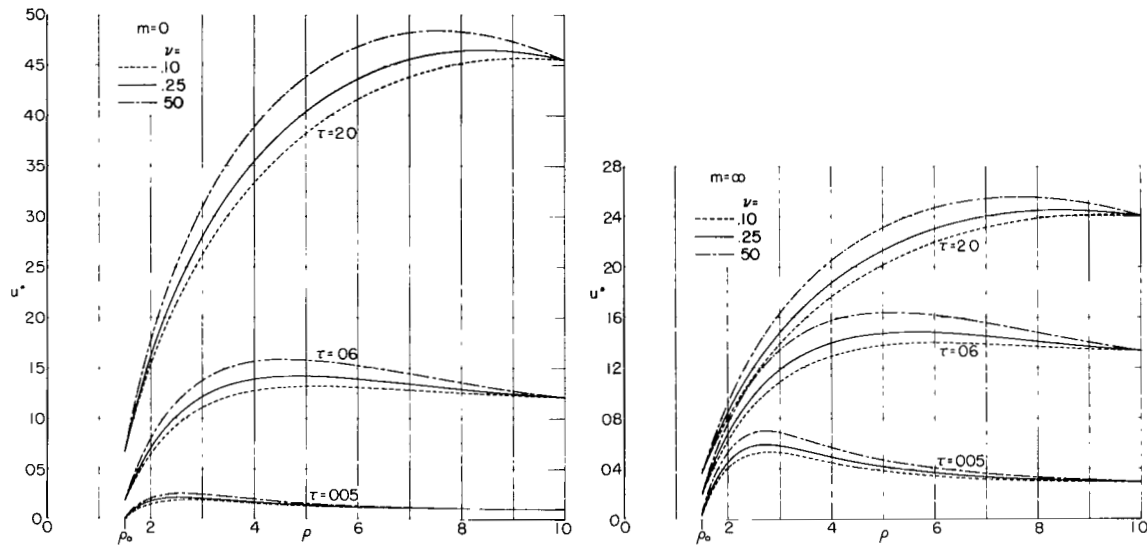


Figure 13.- Effect of Poisson's ratio ν on displacement $u^*(\rho_0 = 0.15)$.

extreme cases $m = 0, \infty$. In all cases, the magnitude of the displacement increases with ν . In the most severe heating ($m = \infty$), the change in displacement due to a change in ν is sizable at its maximum, even for the smallest value of τ ($\tau = 0.005$) considered.

Similar results for the stress difference $(\sigma_r' - \sigma_\theta')$ in the fixed boundary situation appear in figure 14. Here, for $\tau = 0.005$ and $m = \infty$, the effect of altering ν does not appear to be proportionately as great as it was for the displacement results shown above.

The Influence of Wall Thickness

The differences between the solutions under various heating inputs and restraint conditions for differing values of the geometrical parameter ρ_0 are somewhat more difficult to predict than those found in the parameter surveys

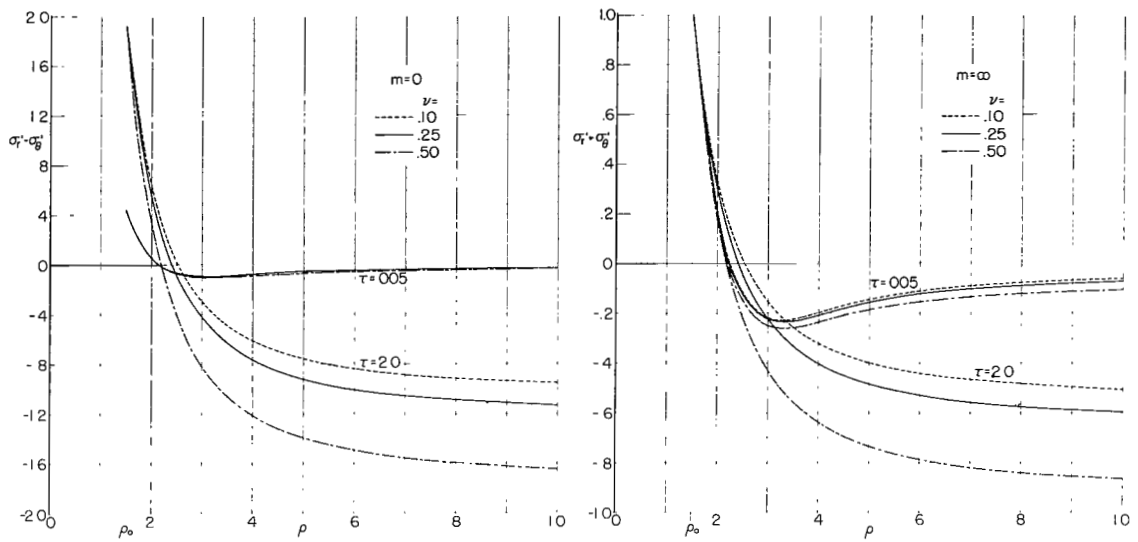


Figure 14.- Effect of Poisson's ratio ν on maximum shearing stress $(\sigma_r^* - \sigma_\theta^*)$ ($\rho_0 = 0.15$).

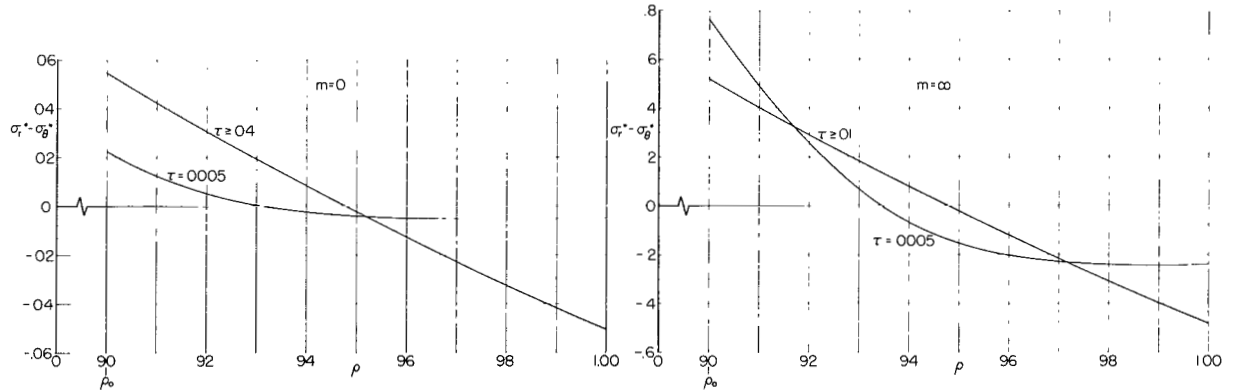


Figure 15.- Variation of maximum shear $(\sigma_r^* - \sigma_\theta^*)$ in thin-walled disk ($\rho_0 = 0.90$, $\nu = 0.25$).

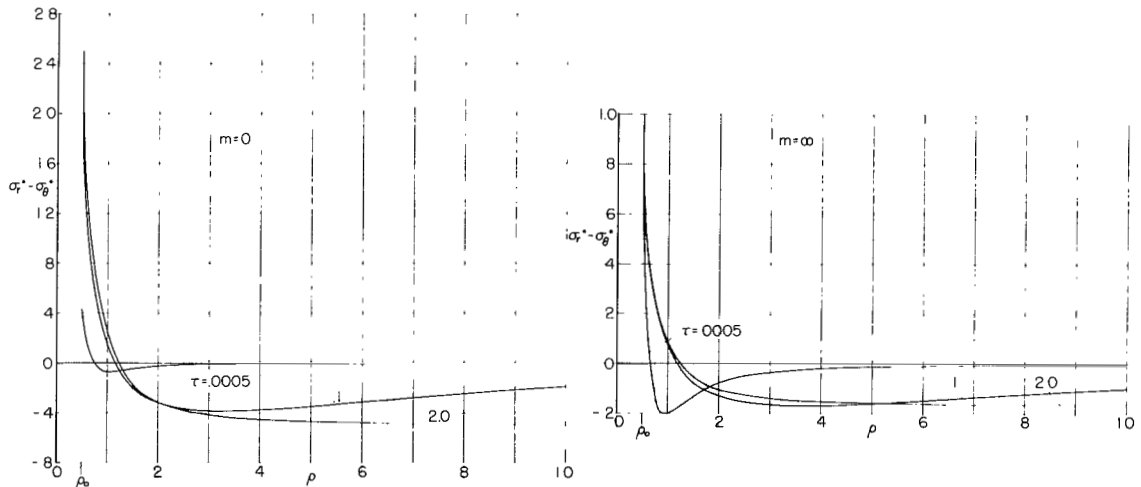


Figure 16.- Variation of maximum shear $(\sigma_r^* - \sigma_\theta^*)$ in thick-walled disk ($\rho_0 = 0.05$, $\nu = 0.25$).

considered above. First, figures 15 and 16 show stress differences for widely different wall thicknesses ($\rho_0 = 0.05$ and 0.90) for a free outer boundary, and for the extreme heating conditions $m = 0, \infty$. In the case of the thin wall ($\rho_0 = 0.90$, fig. 15), the steady-state distributions appear nearly linear for both heating conditions, while the starting distributions ($\tau = 0.0005$) are somewhat simpler than those given previously for $\rho_0 = 0.15$; that is, no trace of an internal extremum in stress difference remains.

In figure 16, the results for stress difference in a very thick ring are given. Here the stress gradient near the inner surface is much greater than in the thin-ring of figure 15. A definite interior extremum exists for small τ , and there is a greater concentration of the stress near the inner surface at the initiation of heating.

Figures 17 and 18 show the quantities corresponding to those in figures 15 and 16, only for the stress-boundary condition of rigid restraint at $\rho = 1$. The character of these figures is analogous to that of the corresponding ones for a free outer boundary, with the expected larger values at $\rho = 1$ due to the rigid restraint.

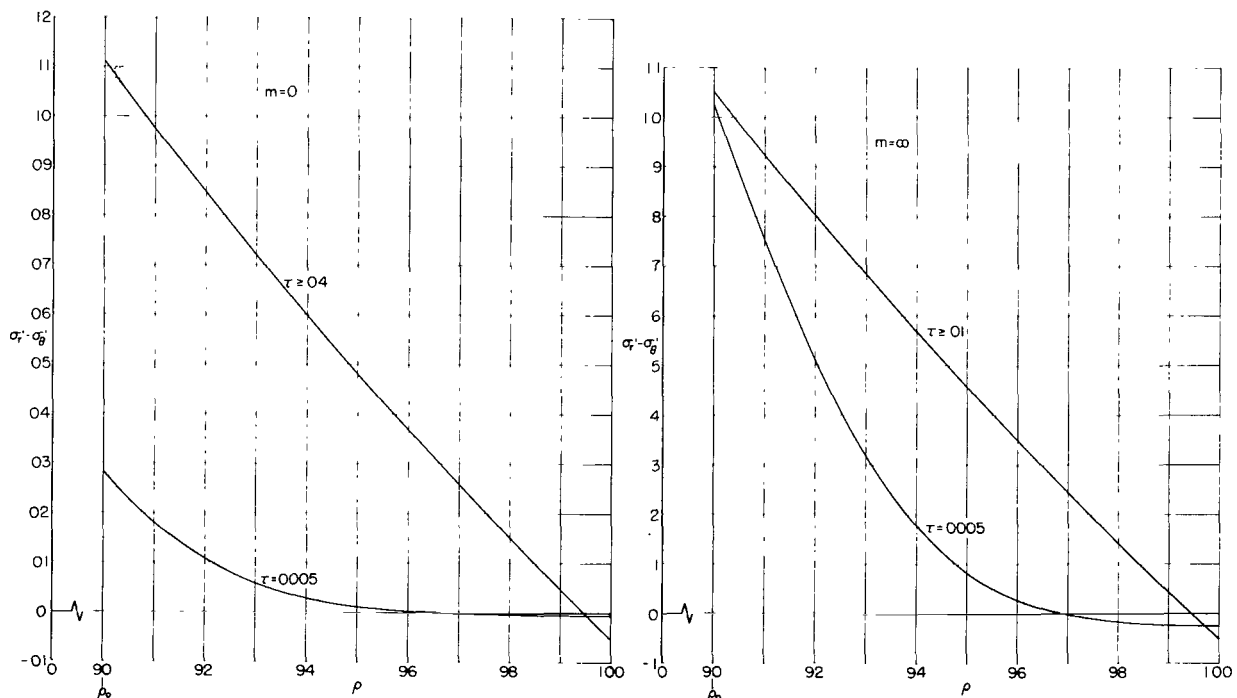


Figure 17.- Variation of maximum shear ($\sigma_r' - \sigma_\theta'$) in thin-walled disk ($\rho_0 = 0.90$, $\nu = 0.25$).

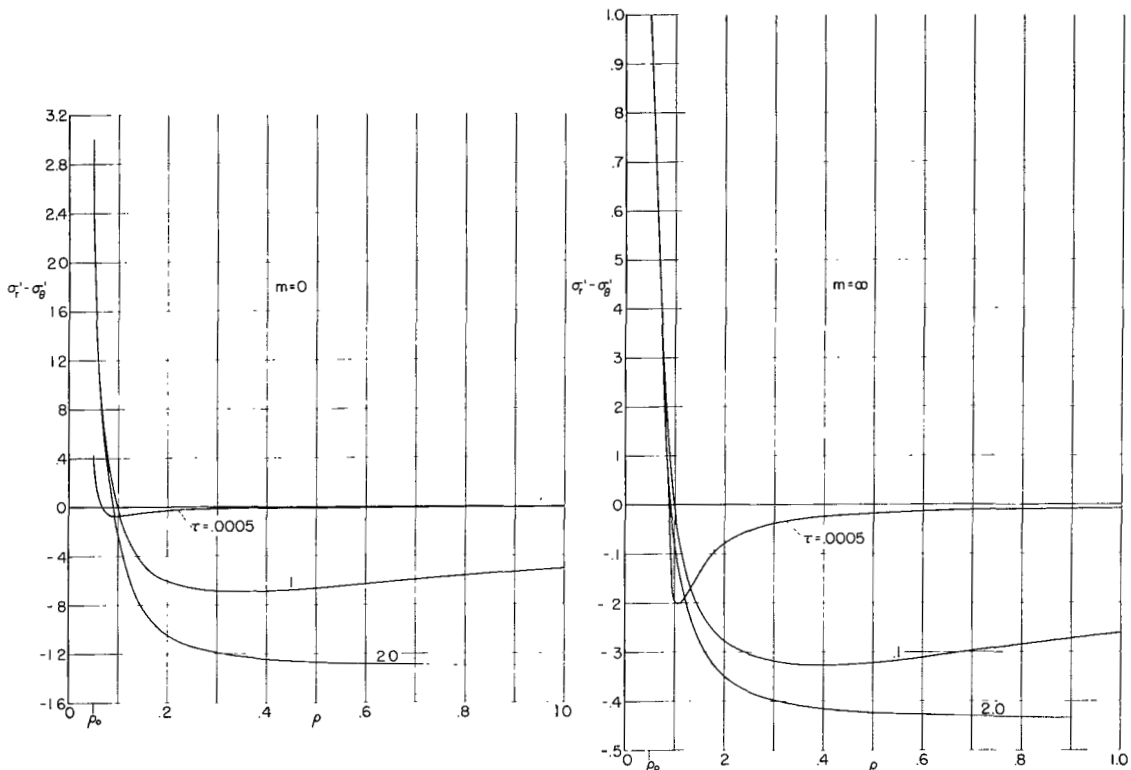


Figure 18.- Variation of maximum shear ($\sigma_r' - \sigma_\theta'$) in thick-walled disk ($\rho_0 = 0.05$, $\nu = 0.25$).

CONCLUDING REMARKS

The present calculations should be useful in determining heating which will keep the stresses below some allowable maximum, as illustrated for other configurations by Heisler in reference 1.

The thermal stresses can become considerable, as the following example will show. For the case shown in figure 7, the maximum stress is given by the value of σ_θ^* at the inner wall in the steady state. It is

$$|\sigma_{\max}| = (0.5)\alpha(T_0 - T_1)E$$

For several materials, such as aluminum or steel, the expansion coefficient α has a value roughly $1 \times 10^{-5}/^\circ\text{K}$ to $2 \times 10^{-5}/^\circ\text{K}$. If the temperature difference is $T_0 - T_1 = 200^\circ\text{K}$, the maximum stress is in the range 1×10^{-3} to 2×10^{-3} . (If the object considered is a pipe rather than a disk, this stress is divided by $1 - \nu$. For the materials mentioned, this amounts to taking about $4/3$ the above results.)

Now, as discussed by Nádai in reference 13(ch. 13), the various factors of dependence of material constants upon temperature and the onset of plastic flow should be taken into account when thermal stresses become severe. If it is desired to keep the stresses below the level at which these new effects enter, the calculations above will serve to define limits on the heating, or dimensions, or other parameters which will so confine these thermal stresses.

Ames Research Center
National Aeronautics and Space Administration
Moffett Field, Calif., Sept. 17, 1965

APPENDIX

SYMBOLS

| | |
|-------------------------|--|
| a, b | outer and inner radii of annular disk or hollow cylinder |
| $B_o(z)$ | $I_o(z)K_o(q) - I_o(q)K_o(z)$ |
| $B_1(z)$ | $I_1(z)K_o(q) + I_o(q)K_1(z)$ |
| d | $(\rho_o - 1)/\rho_o$ (eq. (21)) |
| E | Young's modulus |
| h | surface heat-transfer coefficient (eq. (4c)) |
| $I(\rho, \rho_o; \tau)$ | integral arising in stress calculation (eq. (10d)) |
| I_o, K_o | modified Bessel functions of zero order, of first and second kinds |
| J_o, Y_o | Bessel functions of zero order of first and second kinds |
| k | thermal conductivity |
| m | Biot number, hb/k |
| p | Laplace transform variable |
| p_o, p_o^* | internal pressure and dimensionless internal pressure |
| q | $p^{1/2}$ |
| r | radial coordinate |
| t | time |
| T | temperature |
| T_A, T_B, T_C | boundary conditions, equations (4) |
| T_o | temperature of medium in $r < b$ |
| T_1 | initial temperature of solid |
| u | displacement in thermally strained body |
| v_A | dimensionless temperature ratio, $(T_A - T_1)/(T_o - T_1)$ |

| | |
|---------------------------|--|
| v_B | $(T_B - T_1)/(b/k)$ |
| v_C | $(T_C - T_1)/(T_O - T_1)$ if $m > 1$; $(T_C - T_1)/m(T_O - T_O)$ if $m < 1$ |
| z | axial distance along a cylinder |
| α | coefficient of thermal expansion |
| α_n | eigenvalue, equation (7a) |
| β | $(3 + \rho_O)/\rho_O$ (eq. (22)) |
| β_n | eigenvalue, equation (8a) |
| γ | $\frac{1}{8\rho_O}(3 + \rho_O + 8m)$ (see eq. (19)) |
| κ | thermal diffusivity |
| μ_n | eigenvalue (eq. (6a)) |
| ν | Poisson's ratio |
| ρ | dimensionless radial coordinate; r/a |
| ρ_O | b/a |
| σ_r, σ_θ | radial and circumferential stresses |
| σ_z | axial stress |
| τ | dimensionless time variable; $\kappa t/a^2$ |
| $()^*$ | stress condition of free outer boundary |
| $()'$ | stress condition of rigidly restrained outer boundary |

REFERENCES

1. Heisler, M. P.: Transient Thermal Stresses in Slabs and Circular Pressure Vessels. *J. Appl. Mech.*, vol. 20, no. 2, June 1953, pp. 261-269.
2. Boley, Bruno A.; and Weiner, Jerome H.: Theory of Thermal Stresses. John Wiley and Sons, Inc., N. Y., 1960.
3. Boley, B. A.: Thermal Stresses. Proc. First Symposium on Naval Structural Mechanics, Stanford Univ., Stanford, Calif., August 11-14, 1958. J. Norman Goodier and Nicholas J. Hoff, eds., Pergamon Press, N. Y., 1960, pp. 378-406.
4. Dahl, O. G. C.: Temperature and Stress Distribution in Hollow Cylinders. *Trans. ASME*, vol. 46, 1925, pp. 161-208.
5. Gatewood, B. E.: Thermal Stresses in Long Cylindrical Bodies. *Phil. Mag.*, Seventh Series, vol. XXXII, Oct. 1941, pp. 282-301.
6. Kent, Clarence H.: Thermal Stresses in Thin-Walled Cylinders. *Trans. ASME*, vol. 53, 1931, pp. 167-180.
7. Kent, Clarence H.: Thermal Stresses in Spheres and Cylinders Produced by Temperatures Varying With Time. *Trans. ASME*, vol. 54, 1932, pp. 185-196.
8. Lees, Charles H.: The Thermal Stresses in Solid and in Hollow Circular Cylinders Concentrically Heated. *Proc. Roy. Soc. (London)*, Series A, vol. CI, Sept. 1922, pp. 411-430.
9. Jaeger, J. C.: On Thermal Stresses in Circular Cylinders. *Phil. Mag.*, Seventh Series, vol. XXXVI, 1945, pp. 418-428.
10. Trostel, R.: Instationäre Wärmespannungen in Hohlzylindern mit Kreisringquerschnitt. *Ingenieur-Archiv*, XXIV Band, Erstes Heft, 1956, pp. 1-26.
11. Mendelson, A.; and Manson, S. S.: Approximate Solution to Thermal-Shock Problems in Plates, Hollow Spheres, and Cylinders With Heat Transfer at Two Surfaces. *Trans. ASME*, vol. 78, no. 3, Apr. 1956, pp. 545-553.
12. Schmidt, John E.; and Sonnemann, George: Transient Temperatures and Thermal Stresses in Hollow Cylinders Due to Heat Generation. *J. Heat Transfer*, *Trans. ASME*, Series C, vol. 82, Nov. 1960, pp. 273-278.
13. Nádai, Arpád: Theory of Flow and Fracture of Solids. Vol. II, McGraw-Hill Book Co., Inc., N. Y., 1963.
14. Timoshenko, S.; and Goodier, J. N.: Theory of Elasticity. Second ed., McGraw-Hill Book Co., Inc., N. Y., 1951.

15. Goldstein, S.: Some Two-Dimensional Diffusion Problems With Circular Symmetry. Proc. Math. Soc., Second Series, vol. 34, 1932, pp. 51-88.
16. Carslaw, H. S.; and Jaeger, J. C.: Conduction of Heat in Solids. Second ed., Clarendon Press (Oxford), 1959.
17. Watson, G. N.: A Treatise on the Theory of Bessel Functions. Second ed., Cambridge Univ. Press (Cambridge, Eng.), 1958.
18. Carslaw, H. S.; and Jaeger, J. C.: Operational Methods in Applied Mathematics. Second ed., Dover Publications, Inc., 1963. (Reprinted from 1948 Second ed. by Clarendon Press, Oxford)
19. Abramowitz, Milton; and Stegun, Irene A., eds.: Handbook of Mathematical Functions With Formulas, Graphs, and Mathematical Tables. National Bureau of Standards, Appl. Math. Series 55, Washington, D. C., Government Printing Office, 1964.

"The aeronautical and space activities of the United States shall be conducted so as to contribute . . . to the expansion of human knowledge of phenomena in the atmosphere and space. The Administration shall provide for the widest practicable and appropriate dissemination of information concerning its activities and the results thereof."

—NATIONAL AERONAUTICS AND SPACE ACT OF 1958

NASA SCIENTIFIC AND TECHNICAL PUBLICATIONS

TECHNICAL REPORTS: Scientific and technical information considered important, complete, and a lasting contribution to existing knowledge.

TECHNICAL NOTES: Information less broad in scope but nevertheless of importance as a contribution to existing knowledge.

TECHNICAL MEMORANDUMS: Information receiving limited distribution because of preliminary data, security classification, or other reasons.

CONTRACTOR REPORTS: Technical information generated in connection with a NASA contract or grant and released under NASA auspices.

TECHNICAL TRANSLATIONS: Information published in a foreign language considered to merit NASA distribution in English.

TECHNICAL REPRINTS: Information derived from NASA activities and initially published in the form of journal articles.

SPECIAL PUBLICATIONS: Information derived from or of value to NASA activities but not necessarily reporting the results of individual NASA-programmed scientific efforts. Publications include conference proceedings, monographs, data compilations, handbooks, sourcebooks, and special bibliographies.

Details on the availability of these publications may be obtained from:

SCIENTIFIC AND TECHNICAL INFORMATION DIVISION

NATIONAL AERONAUTICS AND SPACE ADMINISTRATION

Washington, D.C. 20546